Journal of Sound and Vibration (2000) **229**(1), 21–64
Article No. jsvi.1999.2481, available online at http://www.idealibrary.com on IDEAL®

ASYMPTOTIC ANALYSIS OF WAVE PROPAGATION ALONG WEAKLY NON-UNIFORM REPETITIVE SYSTEMS

K. P. Burr, M. S. Triantafyllou and D. K. P. Yue

Department of Ocean Engineering, Massachusetts Institute of Technology, Cambridge, MA 02379, *U.S.A.*

(*Received* 9 *December* 1998, *and in final form* 18 *May* 1999)

We consider monochromatic wave propagation along a long, finite, one-dimensional, slightly non-uniform waveguide, whose ends are connected to uniform semi-infinite waveguides. The non-uniformity in the system parameters, which is assumed slowly varying and deterministic, can be tuned to produce a desired scattered wave field or reflection/transmission properties for a broad range of incident wave fields. With this objective in mind, we obtain an analytic solution for wave propagation along repetitive systems, asymptotic in the slowness of the variation of the system parameters. We consider systems governed by a second order finite difference equation and apply the WKB method allowing the index variable to be complex. This allows complex turning points to be considered. The coefficients of the difference equation are represented by their discrete Fourier modes. For complex turning points, we obtain exponentially small reflection, a new result in the context of difference equations. The asymptotic solution, besides revealing how the non-uniformity in the parameters affects wave propagation, furnishes an analytic expression for the system scattering matrix as a function of the system parameters. It also sheds light on the mechanism of localization phenomena for this class of repetitive systems. We also compare the asymptotic results with numerical experiments for large finite one-dimensional non-uniform chains of coupled pendula.

1. INTRODUCTION

A one-dimensional repetitive system is a chain of interconnected subsystems. The subsystems can be identical to each other (uniform repetitive system) or they may vary among each other (non-uniform repetitive system). Our aim is to study wave propagation along repetitive systems consisting of single-degree-of-freedom (d.o.f) subsystems, each interacting with its two nearest neighbors only. The systems are assumed to have a finite non-uniform part embedded in an infinite uniform part. The non-uniformity, i.e., disorder, is assumed to be slowly varying and deterministic. An example of this kind of repetitive system is a one-dimensional chain of coupled pendula. The subsystem is a pendulum coupled with its two nearest neighbors through springs.

0022-460X/00/010021 + 44 $35.00/0

Wave propagation along uniform repetitive systems is possible only for continuous ranges of frequencies called passbands. For wave frequencies in the passband, energy can be transmitted through the system without attenuation, while no energy is transmitted at frequencies that lie outside the system passband. Therefore, we just consider wave frequencies in the system passband. We consider one-d.o.f. subsystem, and hence the system dispersion relation relates the wave frequency with two wave numbers of equal magnitude and opposite sign, which means a left and a right propagating wave mode. A comprehensive discussion on wave propagation on more complex uniform repetitive systems is given in Brillouin [1].

When non-uniformity, i.e., deterministic disorder, is present along a repetitive system, the passband may become narrow, discrete or even disappear. If non-uniformity is present in a long enough part of a repetitive system and distributed in a random fashion, localization phenomena may show up. We can describe localization effects as follows. For wave frequencies inside the uniform system passband, the wave disturbance may show an exponential decay as it travels along the system. As a result, we have strong, or even complete reflection of the wave disturbance incident in the non-uniform part of the system, and the wave disturbance stays localized in space close to the beginning of the non-uniform part of the system. Another feature of the system behavior when localization phenomena are present, is the disproportionately large sensitivity of the system response (shape of natural modes and distribution of natural frequencies) with respect to small variation in the disorder of the system parameters, as pointed out by Pierre [2], Triantafyllou and Triantafyllou [3] and others. This large sensitivity with respect to the system parameters opens the possibility for the design of the non-uniformity of the system parameters to minimize wave transmission, or to allow perfect transmission at desired frequencies, depending upon the intended application. These design problems are one of the motivations for this work, since an analytical expression for the system scattering matrix, even in an asymptotic sense, is a powerful tool to handle those design problems.

Slowly varying non-uniformity allows us to use the WKB method for second order finite difference equations. We focus on very large one-dimensional systems, consisting of hundreds of subsystems. Second order difference equations can be reduced to canonical forms. We chose the canonical form

$$z_{j+1} - 2z_j + z_{j-1} + Q_j z_j = 0, \tag{1}$$

where j is the independent variable and Q_j is a non-uniform sequence that varies slowly with j. Since Q_j is finite, we assume that we can write it as a finite Fourier series. This allow us to extend Q_j for non-integer values of j. We allow j to be a complex variable, which opens the possibility to consider complex turning points, which, to the author's knowledge, were not considered in the literature before. We assume that the sequence Q_j does not have poles or any essential singularity, except at infinity. The WKB method for difference equations is applied similarly as for differential equations. The difference lays in the fact that for difference equations there are two turning point conditions, instead of only one, for differential equations. For pairs of complex conjugate turning points, the WKB method

predicts an exponentially small reflection, whih was known for differential equations, but is a new result for difference equations.

In the next section, we give an outline of previous work on localization phenomena, about the design problems mentioned above and about the WKB method for difference equations. In section 3, we consider an example of a repetitive system, namely a chain of coupled pendula. The non-uniformity appears in the pendula length and it is restricted to a finite part of the chain. We give the governing equation for wave propagation and reduce it to the canonical form (1). In section 4, we discuss the WKB method for second order difference equations and give an asymptotic approximation for the system transfer matrix, that relates the amplitude of the incident and reflected waves with the amplitude of the transmitted wave for the whole non-uniform part of the system. We also discuss localization phenomena through the optics of the WKB method. In section 5, we apply our asymptotic theory to simple non-uniformity configurations. We compare the asymptotic results with direct numeric simulation to access the performance of the asymptotic theory.

2. PREVIOUS WORK

The phenomena of localization has been known in the context of solid-state physics for almost 40 years. Anderson [4] explained many of the transport properties of disorder solids. In the context of structural dynamics only recently localization phenomena had received attention. Hodges [5] was the first to recognize the relevance of localization theory to the context of structural dynamics, and in Hodges and Woodhouse [6] numerical and experimental evidence of localization was provided. Pierre [7] used a statistical approach to evaluate the localization factor. Kissel [8] used the transfer matrix method. He considered the transfer matrices as random quantities with uniform distribution, and he applied Furstenberg's theorem on the limiting behavior of products of the random matrices to evaluate the localization factor. Castanier and Pierre [9] used perturbation techniques to evaluate the Lyapunov exponent (localization factor) of the wave transfer matrix for multi-coupled disordered periodic linear systems. Bouzit and Pierre [10] used a wave transfer matrix approach and statistical perturbation methods to evaluate the localization factor for a multi-span beam with slight randomness in spacing between supports.

Pierre [11, 2] used an eigenvalue/mode perturbation approach to investigate normal-mode localization for disordered structural systems consisting of weakly coupled subsystems. Triantafyllou and Triantafyllou [3] provide a geometric theory to explain frequency coalescence and mode localization. They consider the system eigenvalue problem as a complex mapping between the complex frequency plane and the complex parameter space. They showed that high modal sensitivity, which characterizes localization, is in fact caused by the presence of branch points of the mapping mentioned above in the complex parameter space near the real axis. Therefore, if we want to maximize the localization for a given system, we need to search for the branch points of the mapping where natural frequencies coalesce. The projection of the branch point with smaller imaginary part on the real axis should give the parameter configuration for which normal modes show some

degree of localization. This configuration of non-uniformity should minimize transmission for the whole system passband. Therefore, the geometric theory of Triantafyllou and Triantafyllou [3] provides an approach to the design problem for minimum transmission for systems of small/medium size. For large systems, consisting of hundreds of elements, the search for the branch points where natural frequencies coalesce becomes too complex. Results from the WKB method for second order difference equations may be more suitable.

The design problem mentioned in the introduction was seldom addressed in the literature [12–14]. Keane and Manohar [12] considered the optimum design, from an energy flow point of view, of two axially vibrating rods which are each composed of 20 piecewise uniform sections. Gopalkrishna [13] minimized wave transmission for system with a small number of d.o.f. and weak coupling. He optimized (maximized) the exponential decay constants of the system normal modes in terms of the system parameters to achieve his design objectives. Langley [14] considered non-uniform one-dimensional repetitive systems embedded in infinite uniform systems. He provided tools to design structural filters which might block or allow wave transmission.

The application of the WKB method to second order finite difference equations dates back as early as 1949, according to reference [15], which gives an account of the literature about the WKB method for difference equations before 1977. Early applications were usually in quantum mechanics. Braun [15] proposed a new method to obtain the Liouville–Green formulas and analyzed the matching condition at both simple and singular real turning points. Wilmott [16] considered also matching conditions for simple real turning points. Error bounds for the Liouville–Green formula for the discrete WKB method are discussed in references [17, 18]. The most recent applications of the discrete WKB method are asymptotic for orthogonal polynomials with slowly varying coefficients [17, 19]). Costin and Costin [20] considered recurrence relations of large finite order. They use a matrix formulation and develop connection formulas for simple turning points. Instead of solving an approximate difference equation in the neighborhood of a turning point, they approximate the recurrence relation by a differential equation and obtained connection formulas using this approach.

3. ONE-DIMENSIONAL CHAIN OF COUPLED PENDULA

We consider a one-dimensional chain of coupled pendula where each pendulum is coupled to its two nearest neighbors by linear springs of constant k. We assume that the length of the pendula is non-uniform for a finite part of the chain. The mass of the jth pendulum is denoted as m and its length is given as $(1 + \varepsilon_j)\, l$, where l is a reference length. The mass m and the spring constant k do not vary along the chain. The governing equation for the jth pendulum is a result of the balance of the inertia force with gravity force and the forces applied by the two nearest neighbors. In non-dimensional form, we obtain

$$\ddot{z}_j + \frac{1}{1 + \varepsilon_j} z_j - R\,[z_{j+1} - z_j] + R\,[z_j - z_{j-1}] = 0, \tag{2}$$

where $R = kl/mg$ is the coupling parameter and g is the acceleration due to gravity. The first term in equation (2) corresponds to the inertia force, the second corresponds to the gravity force, the third term is the force applied by pendulum $j+1$, and the last term is the force applied by pendulum $j-1$. We consider a monochromatic wave of frequency ω incident on the non-uniform part of the chain. In this case the time dependence is given by

$$\exp(\mathrm{i}\omega t) \tag{3}$$

and the governing equation (2) assumes the form

$$-R\, z_{j+1} + \left(\frac{1}{1+\varepsilon_j} + 2R - \omega^2\right) z_j - R\, z_{j-1} = 0 \tag{4}$$

which is the governing equation for monochromatic wave propagation along the chain of pendula. Next, we illustrate how to reduce a general second order difference equation to the canonical form (1). We consider a general equation, as follows:

$$a_j(x, y)z_{j+1} + b_j(x, y)z_j + c_j(x, y)\, z_{j-1} = 0, \quad \text{for } j_0 < j < j_0 + M, \tag{5}$$

and for $j < j_0$ and for $j > j_0 + M$, the coefficients in equation (5) are constants. For $j_0 \leqslant j \leqslant j_0 + M$, $a_j(x, y)$, $b_j(x, y)$ and $c_j(x, y)$ are the non-constant coefficients, which depend on the parameters x and y, and do not have any singularity, besides at infinity. The sequences in equation (5) have size M. To reduce equation (5) to the desired canonical form, we consider the change of variable

$$z_j = \left(\prod_{l=j_0-1}^{j} \beta_l\right) \alpha_j y_j, \quad \text{for } j_0 - 1 < j < j_0 + M, \tag{6}$$

where y_j is the new dependent variable. The sequences β_l and α_j are defined in such a way that the general recurrence relation (5) is reduced to the desired canonical form. The elements of the sequence β_l and α_j are given in terms of the sequences a_j and c_j, as follows:

$$\alpha_j = \frac{1}{c_{j+1}}, \quad \text{for } j \geqslant j_0 - 1;\ \beta_j = 1, \quad \text{for } j_0 - 1 \leqslant j \leqslant j_0; \tag{7}$$

$$\beta_{j+1} = \frac{1}{a_j \beta_j \alpha_{j+1}}, \quad \text{for } j \geqslant j_0. \tag{8}$$

After we apply the change of variable (6) to equation (5), we obtain the desired canonical form (1), where the sequence Q_j is defined in terms of the sequences a_j, b_j and c_j:

$$\begin{aligned} Q_j &= \frac{b_j}{c_{j+1}} + 2, \quad \text{for } j = j_0 \\ &= \frac{b_j}{a_{j-1}} + 2, \quad \text{for } j_0 + 1 \leqslant j < j_0 + M. \end{aligned} \tag{9}$$

For the chain of coupled disordered pendula the terms of the sequences a_j, b_j and c_j are given as

$$a_j = -R, \quad b_j = \frac{1}{1+\varepsilon_j} + 2R - \omega^2, \quad c_j = -R. \tag{10}$$

In the canonical form (1), the term Q_j assumes the form

$$\begin{aligned} Q_j &= \frac{1}{-R}\left(\frac{1}{1+\varepsilon_j} + 2R - \omega^2\right) + 2, \quad \text{for } j = j_0 \\ &= \frac{1}{-R}\left(\frac{1}{1+\varepsilon_j} + 2R - \omega^2\right) + 2, \quad \text{for } j \geqslant j_0 + 1. \end{aligned} \tag{11}$$

Equation (11) is derived directly and simply from equations (1) and (4). The general analysis contained in equations (5)–(9) was carried out because the asymptotic theory below was designed to handle general second order difference equations.

In the the next section, we give an outline of the WKB method for second order difference equations.

4. THE WKB METHOD FOR SECOND ORDER DIFFERENCE EQUATIONS

We give an outline of the WKB method for second order difference equations applied to our canonical form (1). As mentioned before, the WKB method for second order difference and differential equations have many features in common, but the main difference lies in the fact that for difference equations we have two turning point conditions, instead of only one as in the case of differential equations. The first step is to obtain the Liouville–Green formulae. The asymptotic solution of equation (1) is a linear combination of the Liouville–Green functions.

4.1. LIOUVILLE–GREEN FUNCTIONS

To obtain the Liouville–Green functions, we proceed in a way similar to reference [15]. Through a change of variable, we transform the canonical form (1) into a non-linear difference equation. We solve it approximately through an iterative process. The solution of the first iteration gives the Liouville–Green functions. The change of variable to consider is

$$z_j = \prod_{l=l_0}^{j} u_l, \tag{12}$$

and if we substitute equation (12) in the canonical form (1), we obtain a discrete version of the Riccati equation for u_l, as follows:

$$u_l^2\left(\frac{u_{l+1}}{u_l}\right) + (Q_l - 2)\, u_l + 1 = 0. \tag{13}$$

We can solve equation (13) as a quadratic equation, and the natural logarithm of u_l follows:

$$\ln u_l = -\tfrac{1}{2}\Delta \ln u_l + \ln\left(-D_l E_l \pm [(D_l E_l)^2 - 1]^{1/2}\right), \tag{14}$$

where the quantities D_l and E_l are defined as

$$D_l = \left(\frac{u_l}{u_{l+1}}\right)^{1/2}, \qquad E_l^2 = \frac{(Q_l - 2)^2}{4} \tag{15, 16}$$

and Δ is the forward difference operator. The last term in equation (14) is the logarithm of a complex number with unitary modulus and phase θ_l, which can be written as

$$\theta_l = \arccos\left\{-E_l \exp\left(-\tfrac{1}{2}\Delta \ln u_l\right)\right\} \quad \text{for } |D_l E_l| < 1, \tag{17}$$

$$\theta_l = -i \cosh^{-1}\left\{-E_l \exp\left(-\tfrac{1}{2}\Delta \ln u_l\right)\right\} \quad \text{for } |D_l E_l| > 1, \tag{18}$$

and equation (14) assumes, the form

$$\ln u_l = -\tfrac{1}{2}\,\Delta \ln u_l \pm \mathrm{i}\theta(l). \tag{19}$$

From equation (19) we develop an iterative scheme to compute approximations for u_l. We assume that the departure of u_l/u_{l+1} from unity is small, so equation (19) simplifies by eliminating the forward difference of the logarithmic term. The expressions of θ_l, equations (17) and (18), also simplify by setting the forward difference of the logarithmic term equal to zero. Then, the zeroth order approximation follows,

$$\ln u_l^{(0)} = \pm \mathrm{i}\theta_l, \tag{20}$$

and here we redefine θ_l, as follows:

$$\cos(\theta_l) = E_l \text{ for } E_l \text{ real and } |E_l| < 1, \cosh(\mathrm{i}\theta_l) = E_l \quad \text{for } E_l \text{ real and } |E_l| > 1, \tag{21}$$

$$\theta_l = -\mathrm{i} \ln(-E_l + \sqrt{E_l^2 - 1}) \quad \text{for } E_l \text{ complex}, \tag{22}$$

where the last expression in equation (21) is the extension of the arccos function to the whole complex j plane, compatible with the second expression in equation (21). Since higher order approximations of $\ln u_l$ are obtained by iterating equation (19), then $\ln u_l^{n+1}$ is given by

$$\ln u_l^{(n+1)} = -\tfrac{1}{2}\Delta \ln u_l^{(n)} \pm \mathrm{i}\theta_l^{(n+1)}, \tag{23}$$

where $\theta_l^{(n)}$ is the Taylor series expansion of equation (17), if $|E_l| < 1$, or equation (18) if $|E_l| > 1$, with respect to the forward difference of the logarithm of u_l, truncated at the nth order term. To obtain the Liouville–Green functions, we need only to iterate to first order. To obtain $\ln u_l^{(1)}$ we need first to obtain $\theta_l^{(1)}$, which

follows:

$$\theta_l^{(1)} = \theta_l \mp \frac{\mathrm{i}}{2} \cot \theta_l \Delta\theta_l \quad \text{for } |E_l| < 1, \tag{24}$$

$$= \theta_l \mp \frac{1}{2} \coth (i\,\theta_l) \Delta\theta_l \quad \text{for } |E_l| > 1. \tag{25}$$

Next, we substitute equations (24) and (25) with the zeroth order approximation (20) in equation (23), and we obtain the first order approximation for $\ln u_l^{(1)}$,

$$\ln u_l^{(1)} = \mp \frac{\mathrm{i}}{2} \Delta\theta_l \pm \mathrm{i} \left\{ \theta_l \pm \frac{\mathrm{i}}{2} \Delta\theta_l \cot \theta_l \right\} \quad \text{for } |E_l| < 1 \tag{26}$$

and

$$\ln u_l^{(1)} = \mp \frac{\mathrm{i}}{2} \Delta\theta_l \pm \mathrm{i} \left\{ \theta_l \pm \frac{\mathrm{i}}{2} \Delta\theta_l \coth (\mathrm{i}\theta_l) \right\} \quad \text{for } |E_l| > 1. \tag{27}$$

Finally, to obtain the first order approximation for z_j, we substitute equations (26) and (27) in the change of variable (12), and we use the Euler–Maclaurin summation formula. We disregard terms of $\mathrm{O}(\Delta)$ and higher. The final result is

$$z_j^{(1)} = D (\sin \theta_j)^{-1/2} \exp \left\{ \pm \mathrm{i} \int_{j_0}^{j} \theta(l) \mathrm{d}l \right\} \quad \text{for } |E_l| < 1, \tag{28}$$

and

$$z_j^{(1)} = D (\sinh (\mathrm{i}\,\theta_j))^{-1/2} \exp \left\{ \pm \mathrm{i} \int_{j_0}^{j} \theta(l)\, \mathrm{d}l \right\} \quad \text{for } |E_l| > 1, \tag{29}$$

which are the Liouville–Green functions for the canonical equation (1). The quantity $\theta(l)$ in equations (27) and (28) is defined by equation (21). Notice that $\theta(l)$ given by equation (21) is the local wavenumber. In the context of the assumptions of the WKB method, the uniform system dispersion relation, actually given by equation (21), is locally valid. This implies that the passband given by the uniform system dispersion relation varies as we go along the chain. As a result, in the context of the WKB assumptions, energy cannot propagate without attenuation along the chain for every wave frequency inside the uniform system passband. Now, energy can propagate without attenuation only for a subset of the uniform system passband so we have an effective passband, which may be an interval or/and some discrete frequencies, the frequencies of perfect transmission. To illustrate the concept of the effective passband, we assume that the non-uniformity varies along the chain in the interval $(-\varepsilon, \varepsilon)$. In Figure 1, we plot the two edges of the uniform system passband (wavenumber θ equals 0 and π) against values of the non-uniformity (variation of the pendulum length) for the chain of coupled pendula. When these lines cross the line of a constant value of the non-uniformity, the interval so defined is the system passband for that specific value of

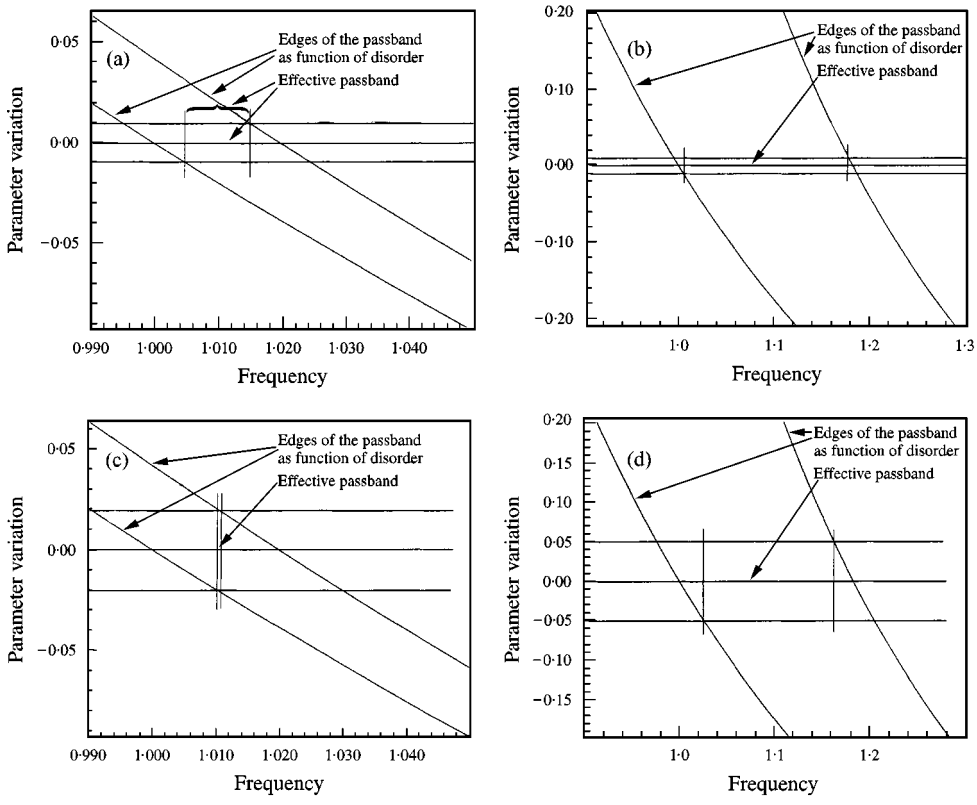

Figure 1. Examples of effective pass band for some values of the coupling parameter R and for some values of the range of the variation of the length of the pendula (%) along the chain: (a) $R = 0{\cdot}01$, 1% variation; (b) $R = 0{\cdot}1$, 1% variation; (c) $R = 0{\cdot}01$, 2% variation; (d) $R = 0{\cdot}1$, 5% variation.

non-uniformity. The intersection of the pass bands for non-uniformities $\pm\varepsilon$ defines the effective passband.

For wave frequencies outside the effective passband, but inside the uniform system passband, the wave disturbance has an exponential decay along the chain length. The width of the effective passband depends on the strength of the coupling parameter and on the amplitude ε of the non-uniformity variation, but for any value of coupling, and no matter how small the non-uniformity is, there is always a boundary layer at both edges of the passband. For wave frequencies inside these boundary layers, the asymptotic theory predicts that the wave disturbance always shows an exponential decay along the length of the chain, staying localized in space. Then for frequencies inside these boundary layers, we have strong localization. For frequencies inside the effective passband, we may have weak localization due to the multiple backscattering which takes place along the system. For long (many wavelengths), slowly varying non-uniform waveguides, the multiple backscattering along the many turning points of the system may be a good description for the multiple backscattering phenomenon which takes places along the system. Therefore, when this approximation is valid, the WKB approach described below should be able to predict weak localization effects.

As $E_l \to +1(-1)$, the wave number θ_l approaches $\pm 0(\pm\pi)$ and the Liouville–Green functions become unbounded, according to equations (28) and (29), and are no longer valid. Points in the complex j plane where $E_j = \pm 1$ are called turning points.

4.2. TURNING POINT CONDITIONS

As pointed out in the last section, the first (second) turning point condition is $E_j = -1$ ($E_j = 1$). In terms of the sequence Q_j of the canonical equation (1), the turning point conditions are given as

$$Q_j - 2 = \mp 2 \to \begin{cases} Q_j = 0, & \text{first condition,} \\ Q_j = 4, & \text{second condition.} \end{cases} \tag{30}$$

For a given sequence Q_j, we describe in Appendix A a procedure on how to obtain the turning points in the complex j plane. Let us denote a turning point that satisfies the first (second) turning point condition (given in equation (30)) as j_{*1} (j_{*2}). In the following, the index k tagged to any constant or used as a superscript denotes the kind of turning point, i.e., whether it satisfies the first ($k = 1$) or second ($k = 2$) turning point condition (30). We consider real and complex first order turning points and second order turning points, which result from the coalescence of a pair of real or complex first order turning points. Higher order and singular turning points may occur, but for the applications of the WKB method we have in mind, they seldom appear. We impose some restrictions on the sequence Q_j, which follows:

- Q_j is real for real values of j.
- θ_j is a finite sequence.
- The extension of sequence Q_j to the complex j plane has no singularity besides at infinity, so for almost the whole complex j plane, the extension of Q_j is an analytic function.

As for differential equations, we can define the Stokes lines. For second order difference equations they are defined as the contours C in the complex j plane such that

$$\Im\left\{\mathrm{i}\int_R^j \theta(l)\,\mathrm{d}l\right\} = 0 \quad \text{with } j \in C, \tag{31}$$

and where R is a turning point that satisfies the first or second turning point condition. The Stokes lines given by equation (31) define regions in the complex j plane (see Figure 2). The asymptotic solution of equation (1) gives by the WKB method is a linear combination of the Liouville–Green functions. As we cross a Stokes line, the appropriate linear combination of the Liouville–Green functions changes, what is called in the literature the Stokes phenomena. Boundary conditions define the appropriate linear combination of the Liouville–Green functions in a region of the complex j plane bounded by Stokes lines, and if we want to know the asymptotic solution in another region of the complex j plane, we have

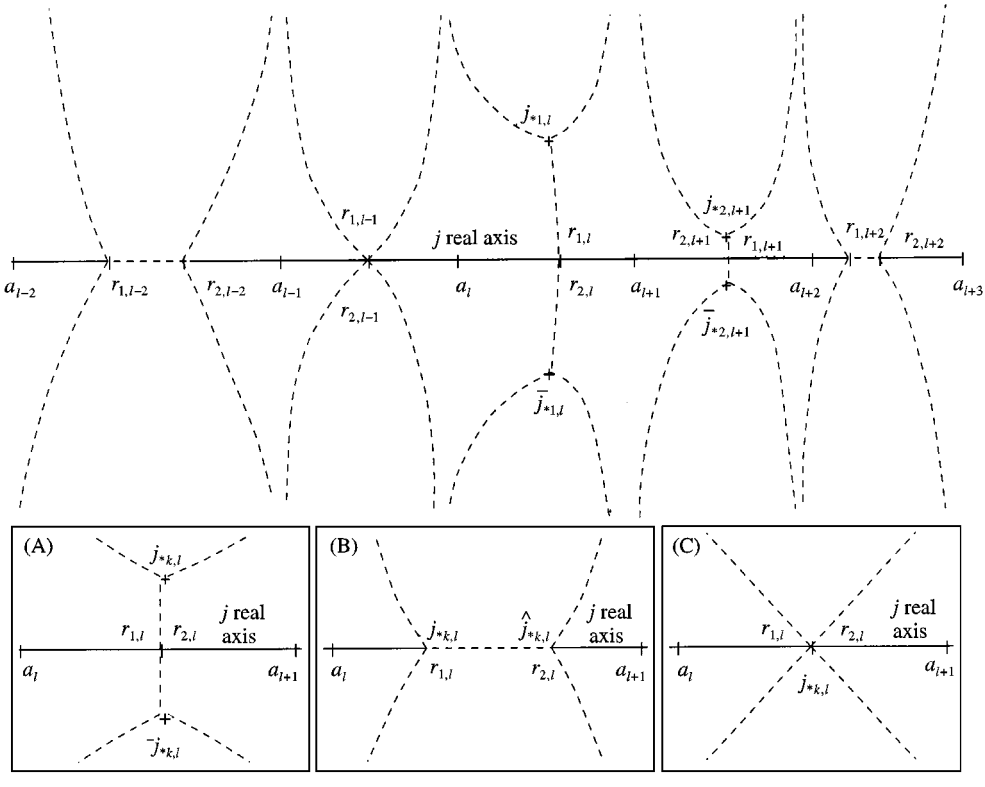

Figure 2. Examples of turning point problems (TPPj, $j = 1, \ldots, 5$) indicated by Stokes lines (– – – –) and boundary points a_l. TPP1: $a_l < j < a_{l+1}$ (pair of complex conjugate turning points $j_{*1,l}$ and $\bar{j}_{*1,l}$; see details in box (A)). TPP2: $a_{l-2} < j < a_{l-1}$ (pair of real turning points $j_{*1,l-2}$ and $\hat{j}_{*1,l-2}$; details box (B)). TPP3: $a_{l+1} < j < a_{l+2}$ (pair of almost coalescent complex conjugate turning points $j_{*2,l+1}$ and $\bar{j}_{*2,l+1}$). TPP4: $a_{l+1} < j < a_{l+2}$ (pair of almost coalescent real turning points $j_{*1,l+2}$ and $\hat{j}_{*1,l+2}$). TPP5: $a_{l-1} < j < a_l$ (second order turning point $j_{2,l-1}$; details box (C)).

to figure out how the linear combination of the Liouville–Green function changes as we cross Stokes lines. To solve this question we develop connection formulae. If we want to connect the solution in two different regions, separated by a Stokes line, we need, first, to see which turning point is common to these two regions, and the necessary connection formula is obtained by solving an approximate from of equation (1), valid in the neighborhood of the turning point in question. Examples of the turning points configurations we are going to deal with are given in Figure 2.

4.3. APPROXIMATE EQUATIONS

In this section, we give the approximation form of equation (1) in the neighborhood of a real or complex first order turning point, and in the neighborhood of a pair of almost coalescing real or complex first order turning points. The case of a second order turning point is the limiting case for almost coalescing turning points.

4.3.1. *Approximate equation for first order turning points*

First, let us discuss the case of real or complex first order turning points. Let us consider j_{*k} a first order turning point. The approximate equation is obtained by a Taylor series expansion of Q_j in equation (1) with respect to j_{*k} to first order. Then equation (1) assumes the form

$$z_{j+1} + (-1)^k\, 2z_j + z_{j-1} + \alpha_k\,(j - j_{*k})\, z_j = 0, \tag{32}$$

where the value of k (1 or 2) denotes which turning point condition is satisfied by turning point j_{*k}, as discussed above. The constant α_k is defined as

$$\alpha_k = \mathrm{d}Q\,(j_{*k})/\mathrm{d}j. \tag{33}$$

The solution of the approximate equation (32) is given in terms of a contour integral; this is discussed in Appendix B.

4.3.2. *Approximate equation for almost coalescing pairs of turning points*

Next, let us consider the case of a pair of almost coalescing real or complex turning points. Let us label this pair of complex conjugate (real) turning points as j_{*k} and $\bar{j}_{*k}$ (j_{*k} and $\hat{j}_{*k}$). For a pair of almost coalescing complex conjugate (real) turning points, we can assume that their real part is the same, so we can write

$$j_{*k} = a_k + \mathrm{i}b_k \quad (j_{*k} = a_k - b_k)$$

and

$$\bar{j}_{*k} = a_k + \mathrm{i}b_k \quad (\hat{j}_{*k} = a_k + b_k), \tag{34}$$

and we assume that $b_k \ll 1$. For real turning points $a_k = |j_{*k} + \hat{j}_{*k}|/2$ and $b_k = |j_{*k} - \hat{j}_{*k}|/2$. To obtain the approximate equation in this case, we expand Q_j in Taylor series with respect to j_{*k} and $\bar{j}_{*k}$ (j_{*k} and $\bar{j}_{*k}$) and disregard terms of $O\,(j - j_{*k})$ and higher. The terms that were not disregarded are now expanded with respect to $\pm\,\mathrm{i}\,b_k (\pm\, b_k)$. We keep only quadratic terms, and then we sum both expansions and divide by two. The approximate equation for this case follows,

$$z_{j+1} + (-1)^k\, 2z_j + z_{j-1} + \psi_k\,[(j - a_k)^2 \pm (b_k)^2]\, z_j = 0, \tag{35}$$

with the constant ψ_k given as

$$\psi_k = \frac{1}{2}\,\frac{\mathrm{d}^2\, Q\,(a_k)}{\mathrm{d}j^2} \tag{36}$$

and the $+\,(-)$ sign in the bracketed term of equation (35) is for the case of a pair of almost coalescing complex conjugate (real) turning points. The approximate difference equation (35) appears in a modified form as the recurrence relation of coefficients of the trigonometric series expansion of the solution of the Mathieu equation. This does not help us in finding a suitable closed-form solution for these difference equations. If we try contour integral solutions, we end up trying to solve a second order differential equation that can be transformed to a Mathieu equation, which does not help us either.

We use a different approach. We approximate equation (35) by a second order differential equation. The second order finite difference operator can be approximated by the second order differential operator in the context of the WKB method assumptions. For the first turning point condition ($k = 1$) the approximate differential form of equation (35), follows:

$$\frac{\mathrm{d}^2 y(j)}{\mathrm{d}j^2} + |\psi_1|[(j - a_1)^2 \pm (b_1)^2]\, y(j) = 0. \tag{37}$$

For the second turning point condition, we make the change of the dependent variable $y_j = \exp(\mathrm{i}\pi j)\, w_j$. For the dependent variable w_j, the approximate differential form of equation (35) with the minus sign is

$$\frac{\mathrm{d}^2 w(j)}{\mathrm{d}j^2} + |\psi_2|[(j - a_2)^2 \pm (b_2)^2]\, w(j) = 0. \tag{38}$$

Let us consider the change of the independent variable,

$$\exp\left(-\mathrm{i}\,\frac{\pi}{4}\right)(4|\psi_k|)^{1/4}\,(j - a_k) = x, \tag{39}$$

which allows us to write equations (37) and (38), respectively, as

$$\frac{\mathrm{d}^2 y}{\mathrm{d}x^2}(x) = (d_1 - \tfrac{1}{4}\,x^2)\, y(x), \quad \frac{\mathrm{d}^2 w}{\mathrm{d}x^2}(x) = (d_2 - \tfrac{1}{4}\,x^2)\, w(x), \tag{40, 41}$$

with $d_k = \pm\,\mathrm{i}\,\sqrt{\mu_k}\,(b_k)^2/4$ (plus sign for complex conjugate turning points and the minus sign for pairs of real turning points), and we define $\mu_k = 4|\psi_k|$. Both equations are related to the parabolic cylinder equation. The functions $D_v(x)$ and $D_v(-x)$ gives a satisfactory solution for the parabolic cylinder equation, when $v \notin N$, in the form given in Bender and Orszag [21, pp. 531, 532]. The solution of equations (37) and (38) in terms of parabolic cylinder functions are

$$\begin{aligned} y(j) = {} & A_1\, D_{\pm(\mathrm{i}/4)\sqrt{\mu_1}(b_1)^2 - 1/2}\left((\mu_1)^{1/4}\,\mathrm{e}^{-\mathrm{i}\pi/4}\,(j - a_1)\right) \\ & + B_1\, D_{\pm(\mathrm{i}/4)\sqrt{\mu_1}(b_1)^2 - 1/2}\left(-(\mu_1)^{1/4}\,\mathrm{e}^{-\mathrm{i}\pi/4}\,(j - a_1)\right), \end{aligned} \tag{42}$$

$$\begin{aligned} w(j) = {} & A_2\, D_{\pm(\mathrm{i}/4)\sqrt{\mu_2}(b_2)^2 - 1/2}\left((\mu_2)^{1/4}\,\mathrm{e}^{-\mathrm{i}\pi/4}\,(j - a_2)\right) \\ & + B_2\, D_{\pm(\mathrm{i}/4)\sqrt{\mu_2}(b_2)^2 - 1/2}\left(-(\mu_2)^{1/4}\,\mathrm{e}^{-\mathrm{i}\pi/4}\,(j - a_2)\right). \end{aligned} \tag{43}$$

For the case of a second order turning point, we proceed in the same way as we did for almost coalescing pairs of first order turning points. We obtain an approximate

difference equation of the form (35), but with $b_k = 0$ and a_k as the second order turning point. We again approximate the second order difference operator in our approximate difference equation by a second order differential operator, which leads to differential equations of the form (40) and (41), but with $d_k = 0$. Therefore, for a second order turning point, the solution of the approximate equation is given by equations (42) or (43) with b_{kl} set to zero. In Appendix C, we give the asymptotic expansions of the solutions of the approximate equations for pairs of almost coalescing real or complex turning points. These asymptotic expansions are used to obtain the connection formulae for these turning point problems.

4.4. CONNECTION FORMULAE

Our objective is to study wave propagation along a repetitive system with slowly varying non-uniformity. Waves propagate only on the real axis of the j complex plane. Therefore, our concern is to see how a given combination of the Liouville–Green functions valid in an interval of the real axis changes as we cross a Stokes line or a real turning point. With this point in mind, we consider the following turning points problems:

- Pair of complex conjugate first order turning points (TPP1).
- Pair of real first order turning points (TPP2).
- Pair of almost coalescing complex conjugate first order turning point (TPP3).
- Pair of almost coalescing real first order turning point (TPP4).
- Second order real turning point (TPP5), which is a particular case of the two cases above.

Our strategy is the following. First, we solve each of these turning point problems alone. We obtain connection formulas for each of them. Second, we use these connection formulas to build the asymptotic solution for repetitive systems with the turning point problems listed above. This will be postponed to the section where we discuss on how to build the asymptotic approximation of the whole system transfer matrix. An example picture of a sequence of turning point problems with the turning point problems listed above is given in Figure 2. In the following, if we refer to a specific turning point problem contained in the list of turning points problems above, we use the symbol TTPj ($j = 1, \ldots, 5$).

Here, let us concentrate on obtaining the connection formulae for the turning point problems listed above. We consider two boundary conditions. The first one is wave incident from left of the turning point. Let us consider points $a_l < a_{l+1}$ along the real axis of the j plane. At points a_l and a_{l+1} the boundary conditions are applied. We consider also the reference points $r_{1,l}$ and $r_{2,l}$, such that $a_l < r_{1,l} \leqslant r_{2,l} < a_{l+1}$ (see boxes (A), (B) and (C) in Figure 2). The index l used below specifies that we are dealing with the lth turning point problem in a sequence of turning point problems, as illustrated by an example in Figure 2. The other boundary condition to consider is an incident wave from the right of the turning point. Let us formulate these boundary conditions in terms of the Liouville–Green functions. For left incidence, we have the following.

- For $a_l < j < r_{1,l}$, we have an incident plus a reflected wave:

$$\sqrt{\sin(\theta_j)}\, z_j \sim A \exp\left(-\mathrm{i} I(a_l, r_{1,l}) - \mathrm{i} \int_{r_1}^{j} \theta(n)\, \mathrm{d}n \right) + R^- A \exp\left(\mathrm{i} I(a_l, r_{1,l}) + \mathrm{i} \int_{r_{1,l}}^{j} \theta(n)\, \mathrm{d}n \right). \tag{44}$$

- For $r_{2,l} < j < a_{l+1}$, we have a transmitted wave:

$$\sqrt{\sin(\theta_j)}\, z_j \sim T^- A \exp\left(-\mathrm{i} \int_{r_{2,l}}^{j} \theta(n)\, \mathrm{d}n \right). \tag{45}$$

where $I(a, b)$ is defined as

$$I(a, b) = \int_a^b \theta(n)\, \mathrm{d}n, \tag{46}$$

and the coefficient R^- and T^- are, respectively, the reflection and transmission coefficients for left incidence.

For right incidence we have the following.

- For $a_l < j < r_{1,l}$, we have a transmitted wave:

$$\sqrt{\sin(\theta_j)}\, z_j \sim T^+ A \exp\left(\mathrm{i} \int_{r_{2,l}}^{j} \theta(n)\, \mathrm{d}n \right), \tag{47}$$

- For $r_{2,l} < j < a_{l+1}$, we have an incident plus a reflected wave:

$$\sqrt{\sin(\theta_j)}\, z_j \sim A \exp\left(\mathrm{i} I(a_{l+1}, r_{2,l}) + \mathrm{i} \int_{r_{2,l}}^{j} \theta(n)\, \mathrm{d}n \right) + R^+ A \exp\left(-\mathrm{i} I(a_l, r_{2,l}) - \mathrm{i} \int_{r_{2,l}}^{j} \theta(n), \mathrm{d}n \right), \tag{48}$$

where the coefficients R^+ and T^+ are, respectively, the reflection and transmission coefficients for right incidence. For each of the turning point problems, the connection formulae are the expressions for the coefficients $R^\pm$ and $T^\pm$. In Appendix B, we obtain the expression for the coefficient $R^\pm$ and $T^\pm$ for TPP1, and in Appendix C we obtain the expressions for the coefficients $R^\pm$ and $T^\pm$ for cases TPP3, TPP4 and TPP5. For TPP2, we just refer the reader to the literature [15, 16]. In what follows, we just list and discuss the results obtained in Appendices B and C.

4.4.1 *Pair of complex conjugate first order turning points*

For TPP1 (see box (A) in Figure 2) and the boundary conditions given above, we describe the connection problem in Appendix B. Let us define the constant

$\gamma = (-1)^k i/\alpha_{k,l}$. For this case we have that the reference points $r_{1,l}$ and $r_{2,l}$ are such that $r_{1,l} = r_{2,l} = r_l = \Re\{j_{*k,l}\}$ (real part of the pair of complex conjugate turning points). The connection formula follows.

- TPP1 with turning points that satisfies the first turning point condition.
  (1) Left incidence boundary condition:

$$R^- = -\exp(-\mathrm{i}2I(r_l, \bar{j}_{*1,l}) - \mathrm{i}2I(a_l, r_l) - \mathrm{i}(\pi/2)), \quad \text{for } -\pi/2 < \arg\{\gamma\} < \pi/2, \tag{49}$$

$$T^- = \exp(-\mathrm{i}I(a_l, r_l)), \quad \text{for } -\pi/2 < \arg\{\gamma\} < \pi/2, \tag{50}$$

  where $I(a, b)$ is defined by equation (46). The integral $I(r_l, \bar{j}_{*1,l})$ is imaginary and negative, which implies that the reflection coefficient R^- is exponentially small. The integral $I(a_l, r_l)$ is real, so it gives a phase change for the reflection and transmission coefficients. The transmission coefficient has modulus equal to unity. The incident wave suffers an exponentially small reflection, and the transmitted wave has a phase shift with respect to the incident wave.
  (2) Right incidence boundary condition:

$$R^+ = -\exp(+\mathrm{i}2I(r_l, j_{*1,l}) - \mathrm{i}2I(r_l, a_{l+1}) + \mathrm{i}(\pi/2)),$$
$$\text{for } -\pi < \arg\{\gamma\} < \pi/2 \text{ and } \pi/2 < \arg\{\gamma\} \leqslant \pi, \tag{51}$$

$$T^+ = \exp(-\mathrm{i}I(r_l, a_{l+1})), \quad \text{for } -\pi < \arg\{\gamma_{r,l}\} < -\pi/2 \text{ and } \pi/2 < \arg\{\gamma\} \leqslant \pi. \tag{52}$$

  The reflection coefficient is exponentially small due to the integral $I(r_l, j_{*1,l})$ which is imaginary and positive.
- TPP1 with turning points that satisfy the second turning point condition.
  (1) Left incidence boundary condition:

$$R^- = -\exp(-\mathrm{i}2I(r_l, \bar{j}_{*2,l}) - \mathrm{i}2I(a_l, r_l) + \mathrm{i}2\pi\, j_{*2,l} + \mathrm{i}(\pi/2)),$$
$$\text{for } -\pi/2 < \arg\{\gamma\} < \pi/2, \tag{53}$$

$$T^- = \exp(-\mathrm{i}I(a_l, r_l)), \quad \text{for } -\pi/2 = \arg\{\gamma\} < \pi/2. \tag{54}$$

  The coefficient R^- is again exponentially small due to the difference between the integral $I(r_l, j_{*2,l})$ (imaginary and positive) and the term $2\pi j_{*2,l}$ (imaginary part positive). The transmission coefficient T^- has modulus equal to unity.
  (2) Right incidence boundary condition:

$$R^+ = \exp(\mathrm{i}2I(r_l, \bar{j}_{*2,l}) - \mathrm{i}2I(r_l, a_{l+1}) - \mathrm{i}2\pi\, \bar{j}_{*2,l} + \mathrm{i}\,(\pi/2)),$$
$$\text{for } -\pi < \arg\{\gamma\} < \pi/2 \text{ and } \pi/2 < \arg\{\gamma\} \leqslant \pi, \tag{55}$$

$$T^+ = \exp(-\mathrm{i}I(r_l, a_{l+1})), \quad \text{for } -\pi \leqslant \arg\{\gamma\} < -\pi/2 \text{ and } \pi/2 < \arg\{\gamma\} < \pi. \tag{56}$$

4.4.2. *Pair of real first order turning points*

For TPP2 with the pair of real turning points denoted as $j_{*k,l}$ and $\hat{j}_{*k,l}$ (see box (B) of Figure 2) and the boundary conditions given above, we just list results presented in the literature using our notation. The connection formula follows.

- Left incidence boundary condition:

$$R^- = \exp(-\mathrm{i}2I(a_l, j_{*k,l}) + (-1)^k\ \mathrm{i}(\pi/2) + \mathrm{i}2\pi\ j_{*k,l}\ \delta_{2,k}), \tag{57}$$

$$T^- = \exp(-\mathrm{i}I(a_l, j_{*k,l}) - \mathrm{i}I(j_{*k,l}, \hat{j}_{*k,l})). \tag{58}$$

- Right incidence boundary condition:

$$R^- = \exp(-\mathrm{i}2I(\hat{j}_{*k,l}, a_{l+1}) - (-1)^k\ \mathrm{i}(\pi/2) + \mathrm{i}2\pi\ \hat{j}_{*k,l}\ \delta_{2,k}), \tag{59}$$

$$T^+ = \exp(-\mathrm{i}I(\hat{j}_{*k,l}, a_{l+1}) - \mathrm{i}I(j_{*k,l}, \hat{j}_{*k,l})). \tag{60}$$

4.4.3. *Pair of almost coalescing first order complex conjugate or real turning points*

In this section, we give the connection formula for the cases TPP3 and TPP4. For TPP3 the reference points $r_{1,l}$ and $r_{2,l}$ are such that $r_{1,l} = r_{2,l} = \Re\{j_{*k,l}\}$, and for TPP4 we have $r_{1,l} = j_{*k,l} < r_{2,l} = \hat{j}_{*k,l}$, with $j_{*k,l}$ and $\hat{j}_{*k,l}$ representing the pair of real turning points. The quantities b_k and μ_k were defined in section 4.3.2, and here we relabel them, respectively, as $b_{k,l}$ and $\mu_{k,l}$. The connection formulas for a given boundary condition does not change if the turning points satisfies the first or the second turning point condition. Therefore, we distinguish the connection formula with respect to the boundary condition used. In Appendix C, we discuss in detail how these connection formulae were derived. In the expressions below, the upper (lower) sign refers to TPP3 (TPP4). The connection formula follow.

- Left incidence boundary condition:

$$R^- = -\frac{\Gamma(\mp(\mathrm{i}/4)\sqrt{\mu_{k,l}}(b_{k,l})^2 + 1/2)}{\sqrt{2\pi}}\, 2^{\pm\,\mathrm{i}(3/2)\sqrt{\mu_{k,l}}(b_{k,l})^2}\ \mu_{k,l}{}^{\mp(\mathrm{i}/8)\sqrt{\mu_{k,l}}(b_{k,l})^2}$$
$$\times \exp\left(\mp\frac{\pi}{8}\sqrt{\mu_{k,l}}\,(b_{k,l})^2 + \mathrm{i}(\pi/2) - \mathrm{i}2I(a_l, r_{1,l}) + \mathrm{i}2\pi\ r_{1,l}\delta_{k,2}\right), \tag{61}$$

$$T^- = \frac{\Gamma(\mp(\mathrm{i}/4)\sqrt{\mu_{k,l}}(b_{k,l})^2 + 1/2)}{\sqrt{2\pi}}\, 2^{\pm\,\mathrm{i}(3/2)\sqrt{\mu_{k,l}}(b_{k,l})^2}\ \mu_{k,l}{}^{\mp(\mathrm{i}/8)\sqrt{\mu_{k,l}}(b_{k,l})^2}$$
$$\times \exp\left(\pm\frac{\pi}{8}\sqrt{\mu_{k,l}}\,(b_{k,l})^2 - \mathrm{i}I(a_l, r_{1,l})\right). \tag{62}$$

For the case TPP3 (TPP4) the reflection (transmission) coefficient is an exponentially small quantity which has $1/\sqrt{2}$ as its maximum value. The transmission (reflection) coefficient varies from $1/\sqrt{2}$ to one. These formulas are useful only for small values of the parameters $b_{k,l}$ and $\mu_{k,l}$. Small values of $b_{k,l}$ implies that the turning points are very close to each other, almost coalescing, and small values of $\mu_{k,l}$ implies that the sequence Q_j varies very slowly.

- Right incidence boundary condition:

$$R^+ = -\frac{\Gamma(\mp(\mathrm{i}/4)\sqrt{\mu_{k,l}}(b_{k,l})^2 + 1/2)}{\sqrt{2\pi}}\, 2^{\pm \mathrm{i}(3/2)\sqrt{\mu_{k,l}}(b_{k,l})^2}\ \mu_{k,l}{}^{\mp(\mathrm{i}/8)\sqrt{\mu_{k,l}}(b_{k,l})^2}$$

$$\times \exp\left(\mp \frac{\pi}{8}\sqrt{\mu_{k,l}}\,(b_{k,l})^2 + \mathrm{i}(\pi/2) - \mathrm{i}2I(r_{1,l},\, a_{l+1}) - \mathrm{i}2\pi\, r_{2,l}\, \delta_{k,2}\right), \tag{63}$$

$$T^+ = \frac{\Gamma(\mp(\mathrm{i}/4)\sqrt{\mu_{k,l}}(b_{k,l})^2 + 1/2)}{\sqrt{2\pi}}\, 2^{\pm \mathrm{i}(3/2)\sqrt{\mu_{k,l}}\,(b_{k,l})^2}\ \mu_{k,l}{}^{\mp(\mathrm{i}/8)\sqrt{\mu_{k,l}}(b_{k,l})^2}$$

$$\times \exp\left(\pm \frac{\pi}{8}\sqrt{\mu_{k,l}}\,(b_{k,l})^2 - \mathrm{i}I(r_{1,l},\, a_{l+1})\right). \tag{64}$$

The expressions for the reflection and transmission coefficients are almost the same as in the previous case. We have just a change in the phase of the reflection and transmission coefficients.

For TPP5, we need to set $b_{k,l}$ equal to zero in the expressions for TPP3 or TPP4, and the desired reflection and transmission coefficients follows.

4.4.4. *Improvement of the asymptotic results for reflection and transmission coefficients*

For TPP1, the WKB method gave the transmission efficient of modulus equal to unity and an exponentially small reflection coefficient. For the case TPP2, we have the opposite situation, i.e., exponentially small transmission and reflection coefficient of modulus equal to unity. We can improve the estimate for the transmission coefficient in the case of TPP1, and for the reflection coefficient in the case of TPP2, by making use of some quantity that depends on the solutions of equation (1) and is constant (does not depend on the independent variable j). If the reflection (transmission) coefficient is exponentially small, we can use the quantity mentioned above to estimate the modulus of the transmission (reflection) coefficient. An example of this quantity is

$$\bar{z}_j z_{j+1} - z_j \bar{z}_{j+1} = \text{constant}, \tag{65}$$

where z_j is the solution of equation (1) and where $\bar{z}_j$ is the complex conjugate of z_j. We want to use equation (65) to obtain a relation between the reflection and transmission coefficients. We consider the boundary condition of left incidence

given by equations (44) and (45). If we substitute equation (44) into equation (65), we have the following.

- For j real and $a_l < j < r_{1,l}$,

$$\frac{2A^2}{\sqrt{\sin(\theta_j)\ \sin(\theta_{j+1})}}\{-\sin(I(j, j+1)) + |R^-|\sin(I(j, j+1))\} = \text{constant}. \tag{66}$$

- For j real and $r_{2,l} < j < a_{l+1}$,

$$\frac{2A^2\ |T^-|^2}{\sqrt{\sin(\theta_j)\ \sin(\theta_{j+1})}}\{-\sin(I(j, j+1))\} = \text{constant}. \tag{67}$$

We can subtract these two relations, but first we set $j + 1 = r_{1,l}$ in equation (66) and we set $j = r_{2,l}$ in equation (67). We obtain

$$|R^-|^2 + |T^-|^2 \frac{\sqrt{\sin(\theta_{r_{1,l}-1})\sin(\theta_{r_{1,l}})}\sin(I(r_{2,l},\ r_{2,l}+1))}{\sqrt{\sin(\theta_{r_{2,l}})\sin(\theta_{r_{2,l}+1})}\sin(I(r_{1,l}-1,\ r_{1,l}))} = 1. \tag{68}$$

We have that $\sin(\theta(r_{1,l})) = \sin(\theta(r_{2,l}))$ and we can assume that $\sin(\theta(r_{1,l}-1)) = \sin(\theta(r_{2,l}+1))$ and $\sin(I(r_{1,l}-1,\ r_{1,l})) = \sin(I(r_{2,l},\ r_{2,l}+1))$. As a result we can rewrite equation (68) as

$$|R^-|^2 + |T^-|^2 = 1. \tag{69}$$

For the boundary condition of right incidence we can proceed in the same way as we did for the left incidence case and obtain, basically, the same result;

$$|R^+|^2 + |T^+|^2 = 1. \tag{70}$$

Finally, we use equations (69) and (70) to improve the WKB predictions for the reflection and transmission coefficient, as described below.

- *Exponentially small reflection*; for this case we improve the estimate for the transmission coefficient. From equations (69) and (70) the modulus of the transmission coefficient is now given by

$$|T^\pm| = \sqrt{1 - |R^\pm|^2} \tag{71}$$

and we keep the phase given by the WKB method.

- *Exponentially small transmission coefficient*; for this case we improve the estimate for the reflection coefficient. From equations (69) and (70) the modulus of the reflection coefficient is now given by

$$|R^\pm| = \sqrt{1 - |T^\pm|^2} \tag{72}$$

and we keep the phase given by the WKB method.

4.5. ASYMPTOTIC FORM OF THE SYSTEM TRANSFER MATRIX

The objective of this section is to describe how to obtain the transfer matrix that relates the wave disturbance amplitude at the ends of the non-uniform part of a repetitive system. Wave scattering, in the context of the WKB method occurs at the turning points. Therefore, first we describe how to obtain the transfer matrix for the turning point problems listed in section 4.4, and then we give the whole system transfer matrix as a product of the transfer matrices of the turning point problems that may appear along the non-uniform part of the chain. Let us consider points $a_l < r_{1,l} \leqslant r_{2,l} < a_{l+1}$ along the real axis of the j complex plane, as defined at the beginning of section 4.4. For TPP1, TPP3 and TPP5, $r_{1,l} = r_{2,l}$ (see boxes (A) and (C) of Figure 2). If we have TPP2 or TPP4, $r_{1,l} < r_{2,l}$ and they actually are the turning points (see box (B) of Figure 2). In terms of the Liouville–Green functions, the wave disturbance can be written as follows.

- For $a_l < j < r_{1,l}$ we have

$$\sqrt{\sin(\theta_j)}\, z_j \sim C_l \exp\left(-\mathrm{i}\int_{a_l}^{j} \theta_n \,\mathrm{d}n\right) + D_l \exp\left(\mathrm{i}\int_{a_l}^{j} \theta_n \,\mathrm{d}n\right). \tag{73}$$

- For $r_{2,l} < j < a_{l+1}$ we have

$$\sqrt{\sin(\theta_j)}\, z_j \sim C_{l+1} \exp\left(-\mathrm{i}\int_{r_{2,l}}^{j} \theta_n \mathrm{d}n\right) + D_{l+1} \exp\left(\mathrm{i}\int_{r_{2,l}}^{j} \theta_n \mathrm{d}n\right) \tag{74}$$

The transfer matrix for the lth turning point problem relates the wave amplitudes (C_l, D_l) at the boundary point a_l to the wave amplitudes $(C_{l+1},\ D_{l+1})$ at the boundary point a_{l+1}. To obtain the desired transfer matrix, labelled M_l, we consider the boundary conditions of left and right incidence. For left incidence we have

$$(C_l,\ D_l) = (A,\ R^- A)$$

and

$$(C_{l+1},\ D_{l+1}) = (T^- A \exp(-\mathrm{i}I(r_{2,l},\ a_{l+1})),\ 0), \tag{75}$$

and for right incidence we have

$$(C_l,\ D_l) = (0,\ T^+ A)$$

and

$$(C_{l+1},\ D_{l+1}) = (R^+ A \exp(-\mathrm{i}I(r_{2,l},\ a_{l+1})),\ A \exp(\mathrm{i}I(r_{2,l},\ a_{l+1}))). \tag{76}$$

The reflection and transmission coefficients for both boundary conditions were obtained in sections 4.1–4.4 according to the turning point problem in consideration. Therefore, we can assume the reflection and transmission coefficients

above as known. We apply the boundary conditions (75) and (76) to the matrix equation

$$\begin{pmatrix} C_{l+1} \\ D_{l+1} \end{pmatrix} = \begin{bmatrix} M_{l,11} & M_{l,12} \\ M_{l,21} & M_{l,22} \end{bmatrix} \begin{pmatrix} C_l \\ D_l \end{pmatrix} \tag{77}$$

and obtain the matrix elements in terms of the reflection $R^{\pm}$ and transmission $T^{\pm}$ coefficients. The elements of the matrix M_l and its inverse M_l^{-1} follow:

$$M_{l,11} = \left(T^{-} - \frac{R^{-}R^{+}}{T^{+}} \right) \exp(-\mathrm{i}I(r_{2,l}, a_{l+1})), \tag{78}$$

$$M_{l,12} = \frac{R^{+}}{T^{+}} \exp(-\mathrm{i}I(r_{2,l}, a_{l+1})), \tag{79}$$

$$M_{l,21} = -\frac{R^{-}}{T^{+}} \exp(\mathrm{i}I(r_{2,l}, a_{l+1})), \quad M_{l,22} = \frac{1}{T^{+}} \exp(\mathrm{i}I(r_{2,l}, a_{l+1})), \tag{80, 81}$$

and for the inverse matrix,

$$M_{l,11}^{-1} = \frac{1}{T^{-}} \exp(\mathrm{i}I(r_{2,l}, a_{l+1})), \quad M_{l,12}^{-1} = -\frac{R^{+}}{T^{-}} \exp(-\mathrm{i}I(r_{2,l}, a_{l+1})), \tag{82, 83}$$

$$M_{l,21}^{-1} = \frac{R^{-}}{T^{-}} \exp(\mathrm{i}I(r_{2,l}, a_{l+1})), \tag{84}$$

$$M_{l,22}^{-1} = \left(T^{+} - \frac{R^{-}R^{+}}{T^{-}} \right) \exp(-\mathrm{i}I(r_{2,l}, a_{l+1})). \tag{85}$$

We have the transfer matrix for each of the turning point problems listed in section 4, since for each of these problems, we obtained the reflection and transmission coefficients $R^{\pm}$ and $T^{\pm}$. In the context of the WKB method the wave diffraction problem due to the system non-uniformity is replaced by the wave diffraction problem due to the presence of turning points in the complex j plane. For a large system we have a sequence of turning point problems as we travel along the real axis of the j plane. The transfer matrix that relates the wave amplitudes before and after the non-uniform section of the system is given as the product of the transfer matrices for each of the turning point problems encountered as we travel along the real axis of the j plane. Suppose we want to relate the wave amplitudes at the beginning of the non-uniform section a_0 to the wave amplitudes at the end of the non-uniform section a_n. We assume that between a_0 and a_n we have n turning point problems. The transfer matrix relating these two positions follows as the product of the transfer matrices of the turning point problems found between these

two positions:

$$\begin{pmatrix} C_n \\ D_n \end{pmatrix} = \prod_{l=1}^{n} [M_l] \begin{pmatrix} C_0 \\ D_0 \end{pmatrix} \tag{86}$$

or

$$\begin{pmatrix} C_0 \\ D_0 \end{pmatrix} = \prod_{l=n}^{1} [M_l^{-1}] \begin{pmatrix} C_n \\ D_n \end{pmatrix}. \tag{87}$$

The global transmission and reflection coefficients can be obtained from the product of matrices in equations (86) and (87). For left incidence boundary condition on the non-uniform part of the chain, we use the product of matrices (86). The global reflection and transmission coefficient R_G^- and T_G^- for left incidence follows:

$$R_G^- = -\frac{(\prod_{j=1}^{N} [\mathbf{M}_j])_{21}}{(\prod_{j=1}^{N} [\mathbf{M}_j])_{22}} \exp(-\mathrm{i}2\theta\ (a_0)\ a_0), \tag{88}$$

$$T_G^- = -\left(\left(\prod_{j=1}^{N} [\mathbf{M}_j]\right)_{11} \exp(-\mathrm{i}\theta\ (a_0)\ a_0) - \frac{(\prod_{j=1}^{N} [\mathbf{M}_j])_{12}\ (\prod_{j=1}^{N} [\mathbf{M}_j])_{21}}{(\prod_{j=1}^{N} [\mathbf{M}_j])_{22}} \times \exp(\mathrm{i}\theta\ (a_0)\ a_0)\right) \exp(\mathrm{i}\theta(a_N)a_N). \tag{89}$$

For the boundary condition of right incidence, we derived expressions for the global transmission and reflection coefficients R_G^+ and T_G^+ from equation (87), as follows:

$$R_G^+ = -\frac{(\prod_{j=N}^{1} [\mathbf{M}_j^{-1}])_{12}}{(\prod_{j=N}^{1} [\mathbf{M}_j^{-1}])_{11}} \exp(\mathrm{i}2\theta\ (a_N)\ a_N), \tag{90}$$

$$T_G^+ = \left(\left(\prod_{j=1}^{N} [\mathbf{M}_j^{-1}]\right)_{22} - \frac{(\prod_{j=1}^{N} [\mathbf{M}_j^{-1}])_{21}\ (\prod_{j=1}^{N} [\mathbf{M}_j^{-1}])_{12}}{(\prod_{j=1}^{N} [\mathbf{M}_j^{-1}])_{11}}\right) \times \exp(\mathrm{i}\theta\ (a_N)\ a_N - \mathrm{i}\theta(a_0)a_0). \tag{91}$$

We use these expressions to evaluate the global transmission and reflection coefficients, since they are more stable when these asymptotic results (reflection and transmission coefficients) are evaluated numerically.

5. APPLICATION

We compare the asymptotic results obtained in section 4 with numerical simulation. The physical system used to illustrate the performance of the asymptotic theory is a chain of coupled pendula. We gave the governing equation for wave propagation on a chain of coupled pendula in section 3. We consider only the variation of the pendula length as the source of non-uniformity. At first, we give results for systems with only one pair of turning points. Second, we give results for systems with two pairs of turning points. We give asymptotic and numerical results

for the reflection and transmission coefficients as a function of the wave frequencies and size of the non-uniform part of the system.

5.1. SYSTEM WITH ONE PAIR OF TURNING POINTS

The shape of the non-uniformity is assumed to be a flat Gaussian curve, described by

$$\varepsilon_j = \pm A \exp\left(-\frac{(j - M/2 + j_0)^2}{2\sigma^2}\right) \quad \text{for } j_0 < j < j_0 + M, \tag{92}$$

where M is the size of the non-uniform part of the chain and j_0 is where the non-uniform part starts. The amplitude A is chosen such that we have a second order turning point for a specific wave frequency value that we chose. The value of σ is chosen such that we have a smooth transition to the uniform part of the chain. As M increases, the Gaussian become flatter, so the matching between numerical and asymptotic results increases. The $+(-)$ sign in equation (92) gives turning points that satisfy the first (second) turning point condition. For frequencies at the left (right) side of the uniform system passband (see equation (1)), we have a pair of real turning points (TPP2) that coalesce and become a pair of complex conjugate turning points (TPP1). In the following figures, we present the asymptotic and numerical results for the modulus of the reflection and transmission coefficients as function of the incident wave frequency and size of the non-uniform part of the system. The wave frequency ranges over the uniform system passband.

In Figures 3 and 4 we considered left incidence boundary condition. For right incidence, we have the same results as for left incidence due to the symmetry of the shape considered. According to the results in Figures 3 and 4, as the steepness of the non-uniform part decreases, the match between asymptotic and numerical results increases, except for frequencies where the turning points are close to coalesce. This fact lead us to use a different approach for almost coalescing turning points (TPP3 and TPP4), outlined in sections 4.4.3 and 4.4.4. and in Appendix C. We combined the corrected WKB approximation (see section 4.4.5) with the results for two almost coalescing turning points (TPP3 and TPP4) to obtain a better approximation for the modulus of the reflection and transmission coefficients. In Figure 5 we illustrate the asymptotic results for a pair of almost coalescing real (TPP4) and complex turning points (TPP3). We present results for the modulus of the reflection coefficient only for the left incidence boundary condition, as function of wave frequency and steepness of the Gaussian shape. We consider that the pair of turning points satisfies the first turning point condition only. We just show the part of the passband where the modulus of the reflection/transmission coefficients goes from almost one to exponentially small values.

5.2. SYSTEMS WITH TWO PAIRS OF TURNING POINTS

Again, we use a simple shape to illustrate the asymptotic form of the transfer matrix. We consider a shape that has two TPP*j*s. One of the TPP*j* is related to the first turning point condition and the other is related to the second turning point condition. The shape is a sum of two flat Gaussian curves with the same amplitude,

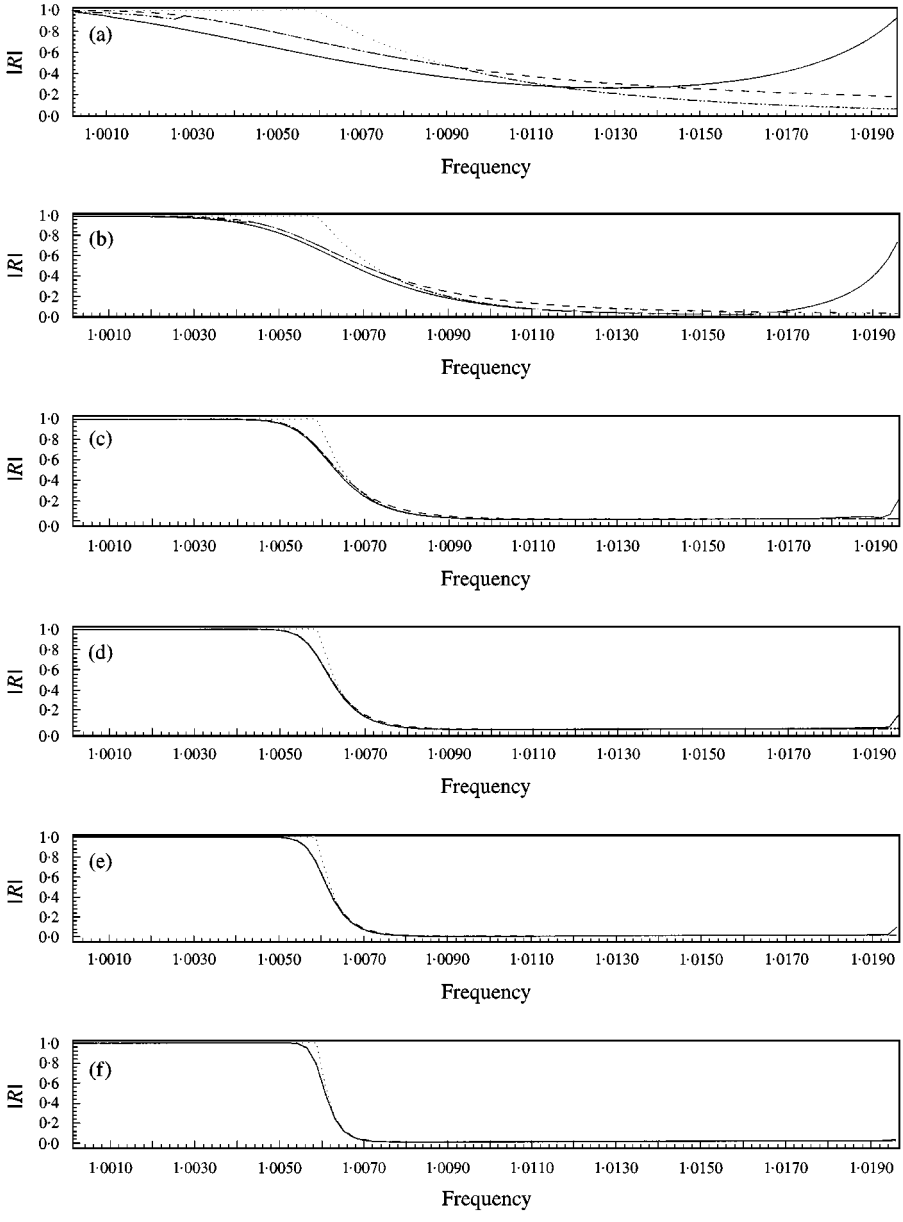

Figure 3. Modulus of the reflection coefficient for left incidence. We have a second order turning point at 30% of the uniform system passband. The turning points satisfy the first turning point condition. Amplitude $A = 0{\cdot}012$; coupling parameter is $R = 0{\cdot}01$; ——, numerical results; . . . , the usual WKB approximation; – – – –, the reflection coefficient given by equations (61) and (63); - ·· – ·· –, a composite approximation. For frequencies close to the frequency for which we have a second order turning point, the reflection coefficient is given by equations (61) and (63). Otherwise, it is given by equations (49) and (57). (a) $M = 11$, (b) 23, (c) 53, (d) 73, (e) 101, (f) 151.

described by

$$\varepsilon_j = \pm A \exp\left(-\frac{(j - M/4 + j_0)^2}{2\sigma^2}\right) \mp A \exp\left(-\frac{(j - 3M/4 + j_0)^2}{2\sigma^2}\right),$$
$$\text{for } j_0 < j < j_0 + M, \tag{93}$$

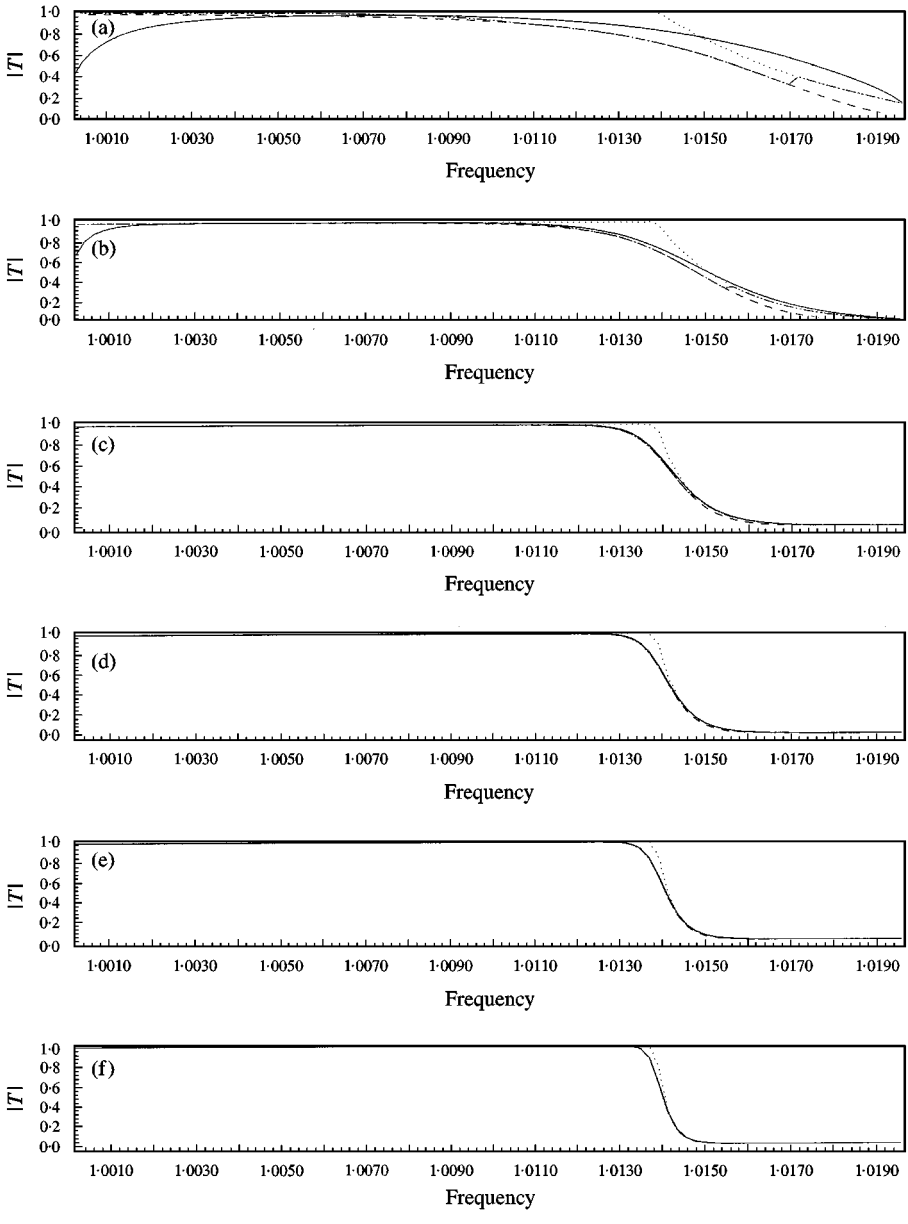

Figure 4. Modulus of the transmission coefficient for left incidence. We have a second order turning point at 70% of the uniform system passband. The turning points satisfy the second turning point condition. Amplitude $A = 0{\cdot}012$; coupling parameter is $R = 0{\cdot}01$; ——, the numerical results; . . . , the usual WKB approximation; – – – –, the transmission coefficient given by equation (64); – ·· – ·· –, a composite approximation. For frequencies close to the frequency for which we have a second order turning point, the transmission coefficient is given by equation (64). Otherwise, it is given by equations (52) and (60). (a)–(f) as in Figure 3.

where M is the size of the non-uniform part of the system and j_0 is where the non-uniform part starts. There is a maximum (minimum) at $M/4$ and a minimum (maximum) at $3M/4$. The amplitude A and σ are chosen as in the previous section. The $+(-)$ sign in equation (93) gives a shape that has a first TPPj

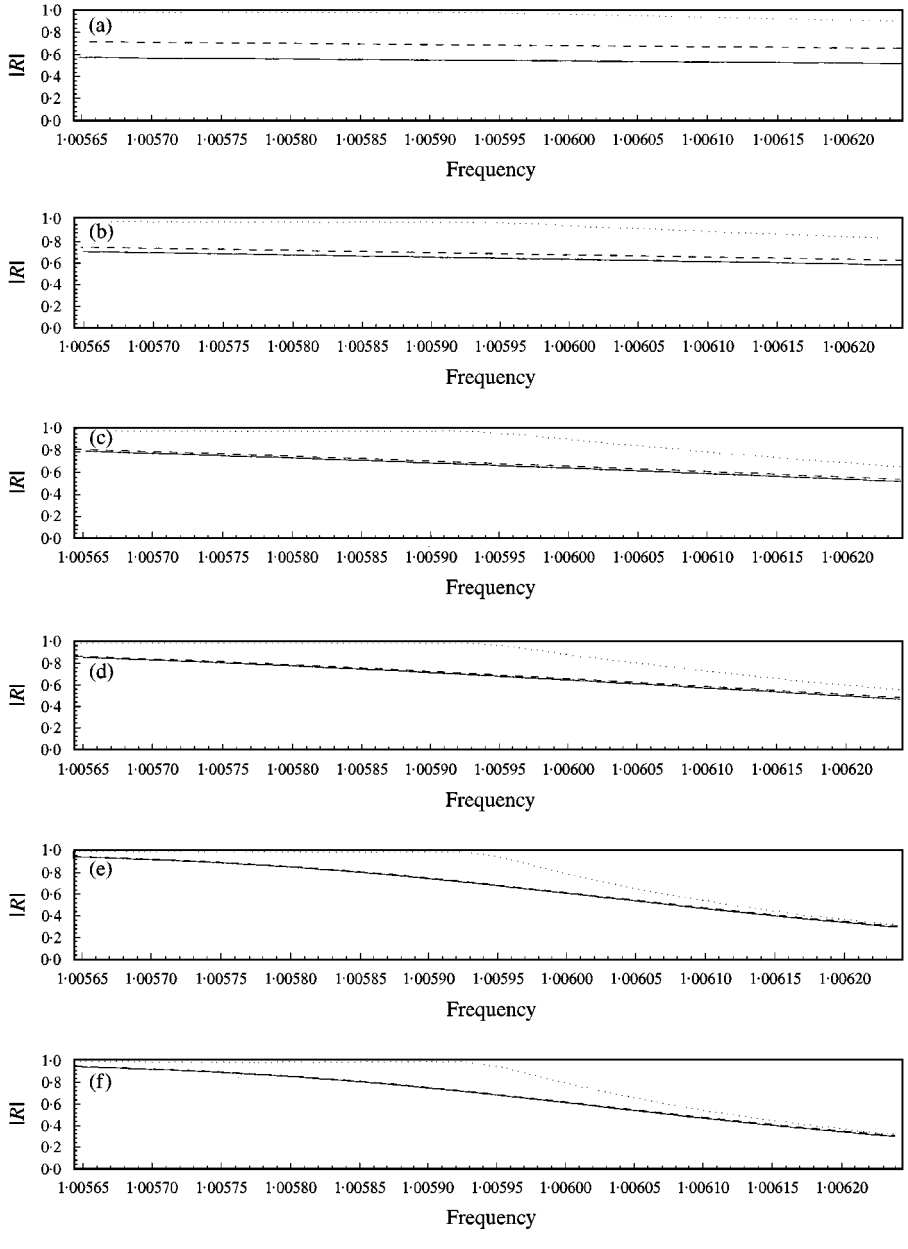

Figure 5. Modulus of the reflection coefficient for left incidence. We have a second order turning point at 30% of the uniform system passband. The turning points satisfy the first turning point condition. Amplitude $A = 0{\cdot}012$; coupling parameter is $R = 0{\cdot}01$; ——, numerical results; – – – –, the reflection coefficient given by equations (61) and (63); …, results given by equations (49) and (57); (a)–(f) as in Figure 3.

associated with the first (second) turning point condition and a second TPPj associated with the second (first) turning point condition. In Figures 6 and 7 we give the modulus of the global reflection and transmission coefficients as a function of wave frequency and size of the non-uniform part of the system. The wave frequency ranges over the uniform system passband. We show results for the left incidence

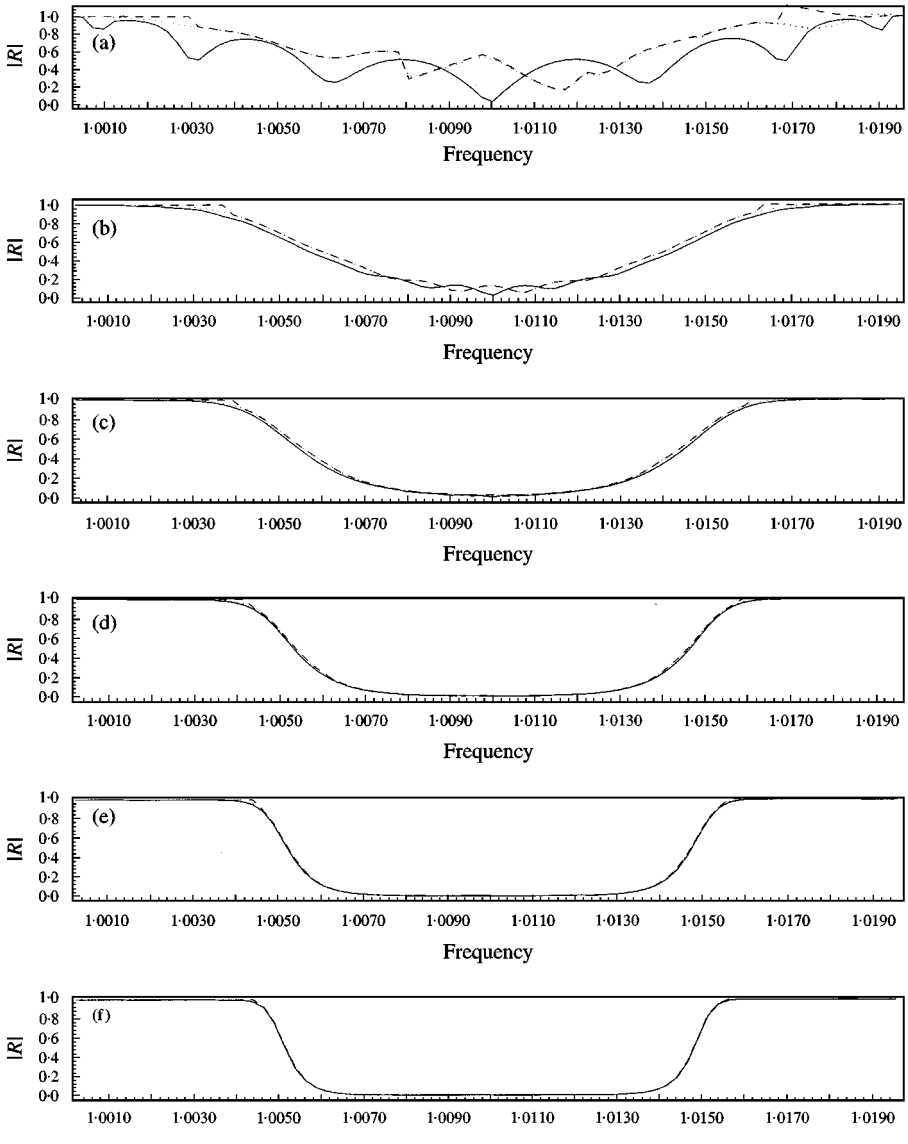

Figure 6. Modulus of the reflection coefficient for left incidence. We have a second order turning point at 25 and 75% of the uniform system passband. Amplitude $A = 0{\cdot}0098$; coupling parameter is $R = 0{\cdot}01$; ——, numerical results; – – – –, the reflection coefficient given by the transfer matrix method. We use the local reflection/transmission coefficients given by the usual WKB approximation. For the … line, we use the local reflection and transmission coefficients corrected by the approximation for almost coalescing pairs of turning points problem. We use this correction when the wave frequency is close to the frequency for which the turning point problem is a second order real turning point. (a) $M = 23$, (b) 47, (c) 73, (d) 103, (e) 153, (f) 203.

boundary condition only. The results for the right incidence boundary condition are similar to the left incidence case due to the symmetry of the shapes considered. For shape (93), we give results for the modulus of the global reflection and transmission in Figures 6 and 7.

The asymptotic results given in Figures 6 and 7 for the reflection and transmission coefficients are given by expressions (88)–(91).

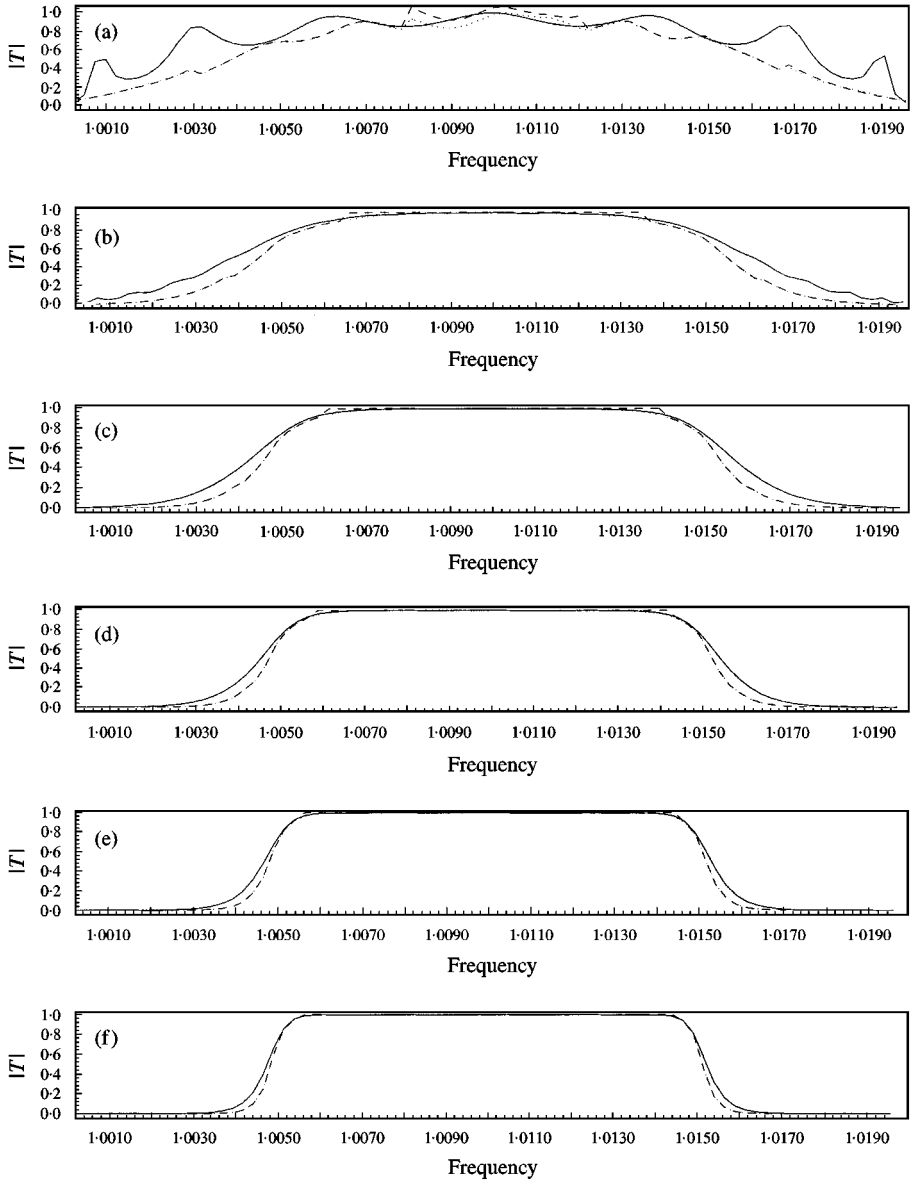

Figure 7. Modulus of the transmission coefficient for left incidence. We have a second order turning point at 25 and 75% of the uniform system passband. Amplitude $A = 0{\cdot}0098$; coupling parameter is $R = 0{\cdot}01$; ——, numerical results; – – –, the transmission coefficient given by the transfer matrix method. We use the local reflection/transmission coefficients given by the usual WKB approximation. For the … line, we use the local reflection and transmission coefficients corrected by the approximation for almost coalescing pairs of turning points. We use this correction when the wave frequency is close to the frequency for which the turning point problem is of second order. (a)–(f) as in Figure 6.

6. DISCUSSION AND CONCLUSIONS

We outline how the asymptotic results can be used to design the slowly varying non-uniformity in a very long chain of coupled pendula to minimize transmission

for the whole system passband. We also comment on some possibilities for future work.

The asymptotic approximations for the reflection and transmission coefficients obtained in section 4 are meaningful only for frequencies inside the uniform system passband, since for other values of wave frequency there is no wave propagation. These asymptotic approximations for the reflection and transmission coefficients are not able to "see" both edges of the passband. Figures 3 and 4 illustrates this fact for a non-uniform chain with only one turning point problem, with turning points that satisfy the first [second] turning point condition (30). As the wave frequency approaches the upper [lower] edge of the uniform system passband, the modulus of the reflection (transmission) coefficient goes to one (zero), but the asymptotic result stays exponentially small (equal to one). In other words, the asymptotic approximation does not model the transition of the modulus of the reflection (transmission) coefficient from exponentially small values to one (one to zero). An example of this kind of non-uniformity is given by equation (92) in section 5.1. For a chain with many turning point problems, we find that some turning points satisfy the first turning point condition (30), and other turning points satisfy the second turning point condition (30). Therefore, for chains with many turning point problems, both uniform system passband edges are modelled properly. The upper (lower) edge is taken into account by turning points that satisfy the first (second) turning point condition (30). We add that turning points that satisfy the first (second) turning point condition (30), model correctly the behavior at the lower (upper) edge of the system effective passband as illustrated in Figures 3 and 4.

The asymptotic approximation for the reflection and transmission coefficients given by the WKB method does not give good results when two turning points start to coalesce. For this situation we considered in a neighborhood of the pair of turning points an approximate form of equation (1) that takes both turning points into account, as described in section 4.3.2 and in Appendix C. This approach seems to be successful as shown in Figure 5. We use these asymptotic results to obtain a better asymptotic approximation for the reflection and transmission coefficients. We combine the usual WKB approximation with the asymptotic results valid when the turning points are almost coalescing, to obtain an asymptotic approximation that gives better results for the whole system passband. Results for this combined approximation are illustrated in Figures 3 and 4.

Regarding localization phenomena, the asymptotic results obtained through the WKB method give some qualitative understanding, as discussed in the end of section 4.1. If the non-uniformity is periodic in space, we have perfect transmission at a discrete set of wave frequencies, with some of them even outside the effective passband. If no periodicity is presented in the non-uniformity, frequencies of perfect transmission are not likely to occur, as pointed out in reference [14]. The problem of perfect transmission was not addressed here. We could have used the asymptotic approximations for the reflection and transmission coefficients to obtain estimates for frequencies of perfect transmission, but due to the complexity of the expressions for the global transmission and reflection coefficients we would have to use a numerical approach to search for the desired frequencies.

Regarding the design problem for minimum transmission, we can use the asymptotic results to design a chain with slowly varying non-uniformity in space. For a maximum allowed amount of non-uniformity at each element of the chain, the idea is to search for the non-uniformity configuration which provides turning points as close as possible to the real axis and has no periodicity. For the problem of a chain of coupled pendula, we have a simple dependence of the sequence Q_j with respect to the wave frequency ω, as illustrated by equation (11). Therefore, by minimizing transmission for a single frequency, located in the middle of the effective passband, it may be sufficient to obtain a non-uniformity configuration that minimizes transmission for the whole effective passband.

We can extend this work in at least two directions. One direction is to extend the WKB method to high order difference equations that arise in the modelling of repetitive system where the interaction of the subsystem is not restricted to the two nearest neighbors. Some work has been done in this direction in reference [20]. Another direction is to extend the analysis done here for second order difference equations to two-dimensional systems of first order difference equations. More interesting systems can be modelled by two-dimensional systems of first order difference equations, like, for example, water waves propagation along a one-dimensional channel with the bottom represented by shelves, or wave propagation along coupled uniform beams with different cross-section.

ACKNOWLEDGMENTS

The first author (Bolsista do CNPq—Brasilia/Brasil) acknowledges financial support from CNPq—Conselho Nacional Cientifico e Tecnologico, of the Ministry for Science and Technology of Brazil under grant 201378/92-2(RN).

REFERENCES

1. L. Brillouin 1953 *Wave Propagatin in Periodic Structures*. New York: Dover Publication, Inc., second edition.
2. C. Pierre 1988 *Journal of Sound and Vibration* **126**, 485–502. Mode localization and eigenvalue loci veering phenomena in disordered structures.
3. M. S. Triantafyllou and G. S. Triantafyllou 1991 *Journal of Sound and Vibration* **150**, 485–500. Frequency coalescence and mode localization phenomena: a geometric theory.
4. P. W. Anderson 1958 *Physical Reviews* **109**, 1492–1505. Absence of diffusion in certain random lattices.
5. C. H. Hodges 1982 *Journal of Sound and Vibration* **82**, 411–424. Confinement of vibration by structural irregularity.
6. C. H. Hodges and J. Woodhouse 1983 *Journal of Acoustic Society of America* **74**, Vibration isolation from irregularity in a nearly periodic structure: theory and measurements.
7. C. Pierre 1990 *Journal of Sound and Vibration* **139**, 111–132. Weak and strong vibration localization in disordered structures: a statistical investigation.
8. G. J. Kissel 1987 *Ph.D. Thesis, Massachusetts Institute of Technology*. Mode localization in disordered periodic structures.

9. M. P. Castanier and C. Pierre 1995 *Journal of Sound and Vibration* **183**, 493–515. Lyapunov exponents and localization phenomena in multi-coupled nearly periodic systems.
10. D. Bouzit and C. Pierre 1995 *Journal of Sound and Vibration* **187**, 625–648. Localization of vibration in disordered multi-span beams with damping.
11. C. Pierre and E. H. Dowell 1987 *Journal of Sound and Vibration* **114**, 549–564. Localization of vibration by structural irregularity.
12. A. J. Keane and C. S. Manohar 1993 *Journal of Sound and Vibration* **168**, 253–284. Energy flow variability in a pair of coupled stochastic rods.
13. G. Rajagopal 1995 *Ph.D. Thesis, Massachusetts Institute of Technology*. Optimal mode localization in disordered, periodic structures.
14. R. S. Langley 1995 *Journal of Sound and Vibration* **188**, 717–743. Wave transmission through one-dimensional near periodic structures: optimum and random disorder.
15. P. A. Braun 1978 *Teoreticheskaya i Matematicheskaya Fizika* **37**, 355–370. WKB method for three-term recursion relations and quasi-energies of an anharmonic oscillator.
16. P. Wilmott 1985 *IMA Journal of Applied Mathematics* **34**, 295–302. A note on the WKB method for difference equations.
17. R. Spigler and M. Vianello 1992 *Journal of Computational and Applied Mathematics* **41**, 105–116. Liouville–Green approximations for a class of linear oscillatory difference equations of second order.
18. R. Spigler and M. Vianello 1994 *SIAM Journal of Mathematical Analysis* **25**, 720–732. Discrete and continuous Liouville–Green–Olver approximations: a unified treatement via Volterra–Stieltjes integral equations.
19. J. S. Geronimo and D. T. Smith 1992 *Journal of Approximation Theory* **69**, 269–301. WKB (Liouville–Green) analysis of second order difference equations and applications.
20. O. Costin and R. Costin 1996 *SIAM Journal of Mathematical Analysis* **27**, 110–134. Rigorous WKB for finite-order linear recurrence relations with smooth coefficients.
21. C. M. Bender and S. A. Orzag 1978 *Advanced Mathematical Methods for Scientists and Engineers*. New York: McGraw-Hill, Inc.
22. K. P. Burr 1998 Massachusetts Institute of Technology. On the asymptotic expansions of the solution of a second order linear difference equation with non-constant linear coefficient.

APPENDIX A: PROCEDURE TO OBTAIN THE TURNING POINTS OF Q_j

For a given sequence Q_j, we describe a procedure of how to obtain the turning points in the complex j plane. We consider real and complex first and second order turning points, which result from the coalescence of a pair of real or complex first order turning points. We impose the restrictions on the sequence Q_j given in section 3.2. The procedure to obtain the turning points is as follows.

- We assume Q_j to be a bounded sequence that oscillates around a fixed value Q_0, so we can write

$$Q_j = Q_0 + \chi_j, \quad \text{for } j = j_0 \text{ to } j_0 + M + 1, \tag{A1}$$

with χ_j given by some functional form for complex values of j. If χ_j is known only at the integer values of j from j_0 to $j_0 + M + 1$, we can represent it by a discrete Fourier series,

$$\chi_j = \sum_{l=1}^{M} \hat{\chi}_l \sin\left[\frac{(j - j_0)\ l\pi}{M + 1}\right], \quad \text{for } j = j_0 \text{ to } j_0 + M + 1, \tag{A2}$$

where $\hat{\chi}_l$ is the discrete Fourier transform of the sequence χ_j. This is the natural way to extend χ_j to the whole complex j plane.

- Maxima and minima of the extension of sequence Q_j to the complex j plane for real j. These points are solutions of the equation

$$\mathrm{d}Q_j/\mathrm{d}j = 0, \quad \text{for } j \text{ real.} \tag{A3}$$

Let us label the solutions of equation (A3) as j^*. We have to check if the points j^* are maxima or minima. With this point in mind we need to evaluate $\mathrm{d}^2Q(j^*)/\mathrm{d}j^2$. If we obtain that

$$\frac{\mathrm{d}^2Q(j^*)}{\mathrm{d}j^2} > 0 \rightarrow j^* \text{ is a minimum}, \quad \frac{\mathrm{d}^2Q(j^*)}{\mathrm{d}j^2} < 0 \rightarrow j^* \text{ is a maximum},$$

let us designate the points j that are maxima as j^{*+} and those that are minima as j^{*-}.

- Search for the real turning points first. To see if there is any real turning point, we just need to check if any of the maxima or minima j^* satisfy

$$Q(j^{*-}) \leqslant 0 \tag{A4}$$

or

$$Q(j^{*+}) \geqslant 4. \tag{A5}$$

If the inequality (A4) is satisfied for some j^{*-}, we have real turning points that satisfy the first turning point condition. If the inequality (A5) is satisfied for some j^{*+}, we have real turning points that satisfy the second turning point condition. These turning points are solutions of

$$Q_0 - 2(1 + (-1)^k) + \chi_j = 0, \quad \text{for } j_0 \leqslant j \leqslant j_0 + M + 1. \tag{A6}$$

We have that $k = 1$ refers to the first turning point condition, and $k = 2$ refers to the second turning point condition. If at each of the maxima j^{*+} or minima j^{*-} one of the inequalities (A4) or (A5) is satisfied, then all the turning points are real. If for some $j^{*\pm}$ an equality of the type (A4) or (A5) is verified, instead of inequality, we have a real second order turning point which coincides with this particular $j^{*\pm}$. If for some $j^{*\pm}$, none of the inequalities (A4) or (A5) are verified, then we have a pair of complex conjugate turning points.

- Search for complex turning points. All the points of the form $j^{*\pm}$ that do not satisfy equations (A4) or (A5) have a pair of complex conjugate turning points associated with it, and we use this fact to obtain the pairs of complex conjugate turning points. Since we are dealing with complex turning points, let us write $j = x + \mathrm{i}y$. A complex turning point satisfies the system of equations

$$Q_0 - 2(1 + (-1)^k) + \Re\{\chi_l\} = 0, \quad \text{with } k = 1, 2, \tag{A7}$$

$$\Im\{\chi_l\} = 0. \tag{A8}$$

To obtain the turning points solutions of the systems of equations (A7)–(A8), we consider the maximum (minimum) j^{*+} (j^{*-}) associated with the turning point we want to obtain. We use the maximum (minimum) j^{*+} (j^{*-}) as a starting value and follow the path described implicitly by equation (A8) for $y > 0$, until equation (A7) is satisfied. This gives one of the desired complex turning point related to the maximum (minimum) j^{*+} (j^{*-}). The other desired turning point is just the complex conjugate of the previous turning point. Complex turning points come as pairs of complex conjugate numbers in the j plane.

The procedure described above can be implemented in a code to find all turning points.

APPENDIX B: CONNECTION FORMULAE FOR A PAIR OF COMPLEX FIRST ORDER TURNING POINTS

In this section, we derive the connection formulae for TPP1. The solution of the approximate form of equation (1), valid in a neighborhood of a first order real or complex turning point, and the leading term of its asymptotic expansion for arbitrary v and $|\gamma| \gg 1$ with $-\pi < \arg\{\gamma\} < \pi$ are given in reference [22]. The results given in reference [22] can be applied directly for the case $k = 1$. The solutions $Hj(\gamma, v)$ for the case $k = 1$ are defined in terms of contour integrals:

$$Hj(\gamma, v) = \int_{C_j} \exp(-2\gamma[-z + \sin z] + \mathrm{i}vz)\, \mathrm{d}z, \quad \text{for } j = 1, 2, 3, \tag{B1}$$

where $v = (j - j_{*k})$. The contours C_j are given in terms of the $\arg\{\gamma\}$, as follows.

- For $\arg(\gamma) \in$ I quadrant, we have C_1 and C_3 asymptotic to $-\pi^- + \mathrm{i}\infty$, C_1 and C_2 asymptotic to $0^- - \mathrm{i}\infty$ and C_2 and C_3 asymptotic to $\pi^- + \mathrm{i}\infty$.
- For $\arg(\gamma) \in$ II quadrant, we have C_1 and C_3 asymptotic to $-\pi^+ + \mathrm{i}\infty$, C_1 and C_2 asymptotic to $0^+ - \mathrm{i}\infty$ and C_2 and C_3 asymptotic to $\pi^+ + \mathrm{i}\infty$.
- For $\arg(\gamma) \in$ III quadrant, we have C_1 and C_3 asymptotic to $-\pi^+ - \mathrm{i}\infty$, C_1 and C_2 asymptotic to $0^- + \mathrm{i}\infty$ and C_2 and C_3 asymptotic to $\pi^+ - \mathrm{i}\infty$.
- For $\arg(\gamma) \in$ IV quadrant, we have C_1 and C_3 asymptotic to $-\pi^- - \mathrm{i}\infty$, C_1 and C_2 asymptotic to $0^+ + \mathrm{i}\infty$ and C_2 and C_3 asymptotic to $\pi^- - \mathrm{i}\infty$.

To deal with the case $k = 2$, we consider the change of variable

$$w_j = z_j \exp(\pm \mathrm{i}\pi j), \tag{B2}$$

which factors out the highest wavenumber wave component and reduces equation (32) for $k = 2$ to the form

$$w_{j+1} - 2w_j + w_{j-1} - \alpha_2 (j - j_{*2}) = 0. \tag{B3}$$

The solution of equation (B3) in terms of contour integrals is given in reference [22], but with $\gamma = \mathrm{i}/\alpha_2$. Therefore, we only need to study the solution of

equation (32) with $k = 1$ and then use the change of variable, equation (B2), to deal with the case $k = 2$.

The solutions $Hj(\gamma, v)$ of the approximate equation (1) will be used in the following to connect a given linear combination of Liouville–Green functions through turning points and Stokes lines. The connection formulae are obtained by matching the asymptotic form of the appropriate function $Hj(\gamma, v)$ for large $|\gamma|$ with the expansion of the Liouville–Green function in terms of the local variable v.

B.1. LOCAL APPROXIMATION OF THE LIOUVILLE–GREEN FORMULA

The second step in obtaining the connection formula is to write the Liouville–Green functions in terms of the local variable, namely α, defined as

$$\alpha = 1 + \mathrm{i}\,(v/2)\gamma. \tag{B4}$$

We consider the boundary conditions of left and right incidences discussed in section 4.4. We write them in terms of the local variable α. The form of the Liouville–Green function in terms of the local variable α changes with respect to the kind of turning point condition (see equation (30)) that is satisfied by the considered turning points.

B.1.1. *Pair of complex conjugate first order turning points*

In this section, we consider two boundary conditions for TPP1, namely left and right wave incidences. We give these boundary conditions as a linear combination of the Liouville–Green functions written in terms of the local variable α. First, we consider TPP1 with turning points (see box (A) in Figure 2) that satisfy the first turning point condition. We use the same notation as in section 4.4.1, namely, we have $a_l < a_{l+1}$ as boundary points, $j_{*1,l}$ and $\bar{j}_{*1,l}$ as the pair of complex conjugate turning points and $r_l = \Re\{j_{*1,l}\}$ $(a_l < r_l < a_{l+1})$ as a reference point in the real axis. For left incidence we have the following.

- For $a_l < j < r_l$ we have an incident plus a reflected wave,

$$\begin{aligned} z_j \sim \frac{1}{(\alpha^2-1)^{1/4}} \{ & A \exp(-\mathrm{i}2\gamma[\sqrt{\alpha^2-1} - \alpha \ln(\alpha + \sqrt{\alpha^2-1})] + \mathrm{i}\frac{\pi}{4} \\ & - \mathrm{i}I(a_l, r_l) - \mathrm{i}I(r_l, \bar{j}_{*1,l})) + R^- A \exp(\mathrm{i}2\gamma[\sqrt{\alpha^2-1} - \alpha \ln(\alpha + \sqrt{\alpha^2-1})] \\ & + \mathrm{i}\frac{\pi}{4} + \mathrm{i}I(a_l, r_l) + \mathrm{i}I(r_l, \bar{j}_{*1,l}))\}. \end{aligned} \tag{B5}$$

- For $r_l < j < a_{l+1}$ we have a transmitted wave,

$$\begin{aligned} z_j \sim \frac{T^- A}{(\alpha^2-1)^{1/4}} \exp(-\mathrm{i}2\gamma[\sqrt{\alpha^2-1} - \alpha \ln(\alpha + \sqrt{\alpha^2-1})] + \mathrm{i}\frac{\pi}{4} \\ - \mathrm{i}I(a_l, r_l) - \mathrm{i}I(r_l, \bar{j}_{*1,l})). \end{aligned} \tag{B6}$$

For the case of left incidence, we approximate the Liouville–Green functions with respect to the complex turning point $\bar{j}_{*1,l}$, since the transmitted wave is exponentially small in the region bounded by the real axis, by the Stokes line that connects both turning points and crosses the real axis and by the Stokes line that emanates from $\bar{j}_{*1,l}$ and goes to infinity for $j > \Re\{\bar{j}_{*1,l}\}$. Since the transmitted wave is exponentially small in the region described above and specified by the boundary conditions, it is uniquely defined in this region. This fact allow us to continue it to other regions with a common turning point ($\bar{j}_{*1,l}$ in this case) by using the asymptotic form of the solution of the approximate form of equation (1), valid in a neighborhood of $\bar{j}_{*1,l}$ (see Figure 2). If the transmitted wave was exponentially large, it would not be defined uniquely by the boundary conditions, since we always can add the other exponentially small Liouville–Green function and the boundary condition is still satisfied. This is actually true for most of the complex j plane. The exceptions are the real axis and the anti-Stokes lines (lines that emanate from the turning points and defined by $\Re\{\int_r^j \theta_n \, \mathrm{d}n\} = 0$, with r as a turning point), where the Louiville–Green functions are of the same order of magnitude. Along these lines, boundary conditions specify uniquely the appropriate linear combination of Liouville–Green functions. Next, we consider the boundary condition of right incidence.

- For $a_l < j < r_l$ we have a transmitted wave,

$$z_j \sim \frac{T^+ A}{(\alpha^2 - 1)^{1/4}} \exp\left(\mathrm{i}2\gamma\left[\sqrt{\alpha^2}1 - \alpha \ln\left(\alpha + \sqrt{\alpha^2 - 1}\right)\right] + \mathrm{i}\frac{\pi}{4} + \mathrm{i}I(r_l, j_{*1,l})\right). \tag{B7}$$

- For $r_l < j < a_{l+1}$ we have an incident plus a reflected wave,

$$\begin{aligned} z_j \sim \frac{1}{(\alpha^2 - 1)^{1/4}} \{ & A \exp(\mathrm{i}2\gamma\left[\sqrt{\alpha^2 - 1} - \alpha \ln\left(\alpha + \sqrt{\alpha^2 - 1}\right)\right] + \mathrm{i}\frac{\pi}{4} + \mathrm{i}I(a_{l+1}, r_l) \\ & + \mathrm{i}I(r_l, j_{*1,l})) + R^+ A \exp(-\mathrm{i}2\gamma\left[\sqrt{\alpha^2 - 1} - \alpha \ln\left(\alpha + \sqrt{\alpha^2 - 1}\right)\right] \\ & + \mathrm{i}\frac{\pi}{4} - \mathrm{i}I(a_{l+1}, r_l) + \mathrm{i}I(r_l, j_{*1,l}))\}, \end{aligned} \tag{B8}$$

and here we chose to expand the Liouville–Green functions with respect to $j_{*1,l}$ for the same reasons mentioned in the case of left incidence. The transmitted wave is exponentially small in the region bounded by the real axis, by the Stokes line that connects both turning points and cross the real axis and by the Stokes line that emanates from $j_{*1,l}$ and goes to infinity for $j < \Re\{j_{*1,l}\}$.

For TPP1 with turning points that satisfy the second turning point condition, we have that the phase term in the Liouville–Green functions is written in terms of the

variable α as

$$\exp(\pm \mathrm{i}\int_r^j \theta_n \mathrm{d}n) \sim$$

$$\begin{cases} \pm \mathrm{i}\pi v + \mathrm{i}2\gamma[\alpha \ln(\alpha + \sqrt{\alpha^2-1}) - \sqrt{\alpha^2-1} & \text{for} \quad \Im\{\alpha\} \geqslant 0, \\ \mp \mathrm{i}\pi v - \mathrm{i}2\gamma[\alpha \ln(\alpha + \sqrt{\alpha^2-1}) - \sqrt{\alpha^2-1} & \text{for} \quad \Im\{\alpha\} < 0. \end{cases} \tag{B9}$$

The term $\pm \mathrm{i}\pi v(\pm \mathrm{i}\pi(j - j_{*2,l}))$ represents the wave with the highest possible wave number. This is due to the fact that in a neighborhood of a turning point that satisfies the second turning point condition, the wave number θ_n is in a neighborhood of the upper edge of the uniform system passband. If we take into account the change of dependent variable (B2), we can factor out the term $\pm \mathrm{i}\pi j$. For waves that propagate to the left, we chose the plus sign in equation (B2), and for waves propagating to the right we chose the minus sign in equation (B2). In terms of the dependent variable w_j, the boundary conditions for left incidence are similar to equations (B5) and (B6). The difference lies in that we consider the turning point $j_{*2,l}$, instead of $\bar{j}_{*2,l}$. The reason is that in the appropriate neighborhood of $j_{*2,l}$, the transmitted wave is exponentially small. In the following four expressions, $r_1 = \Re\{j_{*2,l}\}$. The boundary condition for left incidence, in terms of w_j, follows below.

- For $a_l < j < r_l$ we have an incident plus a reflection wave,

$$\begin{aligned} w_j \sim \frac{1}{(\alpha^2-1)^{1/4}} \{ & A \exp(-\mathrm{i}2\gamma[\sqrt{\alpha^2-1} - \alpha \ln(\alpha + \sqrt{\alpha^2-1})] + \mathrm{i}\frac{\pi}{4} - \mathrm{i}I(a_l, r_l) \\ & - \mathrm{i}I(r_l, j_{*2,l}) + \mathrm{i}\pi j_{*2,l}) + R^- A \exp(\mathrm{i}2\gamma[\sqrt{\alpha^2-1} - \alpha \ln(\alpha + \sqrt{\alpha^2-1})] \\ & + \mathrm{i}\frac{\pi}{4} + \mathrm{i}I(a_l, r_l) + \mathrm{i}I(r_l, j_{*2,l}) - \mathrm{i}\pi j_{*2,l}) \}. \end{aligned} \tag{B10}$$

- For $r_l < j < a_{l+1}$ we have a transmitted wave,

$$\begin{aligned} w_j \sim \frac{T^- A}{(\alpha^2-1)^{1/4}} & \exp(-\mathrm{i}2\gamma[\sqrt{\alpha^2-1} - \alpha \ln(\alpha + \sqrt{\alpha^2-1})] + \mathrm{i}\frac{\pi}{4} \\ & - \mathrm{i}I(a_l, r_l) - \mathrm{i}I(r_l, j_{*2,l}) - \mathrm{i}\pi j_{*2,l}). \end{aligned} \tag{B11}$$

The right incidence boundary condition is similar to equations (B7) and (B8). The difference lies that in this case we consider the turning point $\bar{j}_{*2,l}$ instead of $j_{*2,l}$. The reason is the same as the one mentioned above, i.e., the transmitted wave is exponentially small in the neighborhood of $\bar{j}_{*2,l}$. The boundary condition is as follows.

- For $a_l < j < r_l$ we have a transmitted wave,

$$\begin{aligned} w_j \sim \frac{T^+ A}{(\alpha^2-1)^{1/4}} & \exp(\mathrm{i}2\gamma[\sqrt{\alpha^2-1} - \alpha \ln(\alpha + \sqrt{\alpha^2-1})] + \mathrm{i}\frac{\pi}{4} \\ & + \mathrm{i}I(r_l, \bar{j}_{*2,l}) - \mathrm{i}\pi\bar{j}_{*2,l}). \end{aligned} \tag{B12}$$

- For $r_l < j < a_{l+1}$ we have an incident plus a reflected wave,

$$w_j \sim \frac{1}{(\alpha^2-1)^{1/4}} \{A \exp(\mathrm{i}2\gamma[\sqrt{\alpha^2-1} - \alpha \ln(\alpha + \sqrt{\alpha^2-1})] + \mathrm{i}\frac{\pi}{4}$$

$$+ \mathrm{i}I(a_{l+1}, r_l) + \mathrm{i}I(r_l, \bar{j}_{*2,l}) - \mathrm{i}\pi\bar{j}_{*2,l}) + R^+ A \exp(-\mathrm{i}2\gamma[\sqrt{\alpha^2-1} - \alpha$$

$$\times \ln(\alpha + \sqrt{\alpha^2-1})] + \mathrm{i}\frac{\pi}{4} - \mathrm{i}I(a_{l+1}, r_l) - \mathrm{i}I(r_l, \bar{j}_{*2,l}) + \mathrm{i}\pi\bar{j}_{*2,l})\}. \quad \text{(B13)}$$

The next step is to define the appropriate solution to the locally valid equations (32) ($k = 1$) and (B9). We consider equation (32) as the locally valid equation when turning points of TPP1 satisfy the first turning point condition (30). When turning points of TPP1 satisfy the second turning point condition, we consider the locally valid equation (B9). After we obtain the appropriate solutions of the locally valid equation in terms of the function $H_j(\gamma, v)$, we match these solutions with the expansion of the Liouville–Green formulae given in the section above. The result of the matching process are the reflection/transmission coefficients given by equations (49)–(64). The steps mentioned in this paragraph are given in the next section.

B.2. MATCHING PROCESS

First we give the leading term of the asymptotic expansion of the solution of the locally valid equations (32) and (B9), appropriate for matching with the Liouville–Green formulae for the complex first order turning point. For second order turning points, we already gave the solution of the appropriate locally valid equation in section 4.3.1, so here we only give the asymptotic expansion of this solution.

B.2.1. *Leading term of the asymptotic expansion of the solution of the approximate equation in a neighborhood of a complex first order turning point*

The complex first order turning point satisfies the first or the second turning point condition (30). If it satisfies the first turning point condition, the leading term of the asymptotic expansion of the appropriate solution of equation (32) with $k = 1$ is given below in terms of the functions

$$A(\gamma, v) =$$

$$\frac{1}{2}\sqrt{\frac{\pi}{|\gamma|}} \frac{\exp(-\mathrm{i}2\gamma[\alpha \ln(\alpha + \sqrt{\alpha^2-1}) - \sqrt{\alpha^2-1}] - \mathrm{i}(\pi/4) - (\mathrm{i}/2)\arg\{\gamma\})}{(\alpha^2-1)^{1/4}} \quad \text{(B14)}$$

$$B(\gamma, v) =$$

$$\frac{1}{2}\sqrt{\frac{\pi}{|\gamma|}} \frac{\exp(\mathrm{i}2\gamma[\alpha \ln(\alpha + \sqrt{\alpha^2-1}) - \sqrt{\alpha^2-1}] - \mathrm{i}(\pi/4) - (\mathrm{i}/2)\arg\{\gamma\})}{(\alpha^2-1)^{1/4}}. \quad \text{(B15)}$$

The leading term of the asymptotic expansion for the appropriate solution of (32) with $k = 1$ for $|\gamma| \gg 1$ and $|v| \leqslant |\gamma|$ follows.

- For left incidence boundary condition (turning point $\bar{j}_{*1,l}$):

$$z_j \sim -C\ B(\gamma, v), \quad \text{for } 0 < \arg\{\gamma\} < \frac{\pi}{2} \text{ and } \frac{\pi}{6} < \beta < \frac{\pi}{2}; \tag{B16}$$

$$z_j \sim C(A(\gamma, v) - B(\gamma, v)), \quad \text{for } 0 < \arg\{\gamma\} < \frac{\pi}{2} \text{ and } \frac{\pi}{2} < \beta < \frac{5\pi}{6};$$

$$z_j \sim -CB(\gamma, v), \quad \text{for } 0 \geqslant \arg\{\gamma\} > -\frac{\pi}{2} \text{ and } \frac{\pi}{6} < \beta < \frac{\pi}{2}; \tag{B17}$$

$$z_j \sim C(A(\gamma, v) - B(\gamma, v)), \quad \text{for } 0 \geqslant \arg\{\gamma\} > -\frac{\pi}{2} \text{ and } \frac{\pi}{2} < \beta < \frac{5\pi}{6}.$$

where β is defined by

$$\beta = \arg\{v\} - \tfrac{1}{3} \arg\{\gamma\} \tag{B18}$$

in terms of $\arg(v\}$ and $\arg\{\gamma\}$.

- For right incidence boundary condition (turning point $j_{*1,l}$):

$$z_j \sim -CA(\gamma, v), \quad \text{for } \frac{\pi}{2} \leqslant \arg\{\gamma\} \leqslant \pi \text{ and } \frac{5\pi}{6} < \beta < \frac{7\pi}{6};$$

$$z_j \sim -C(A(\gamma, v) + B(\gamma, v)), \quad \text{for } \frac{\pi}{2} \leqslant \arg\{\gamma\} \leqslant \pi \text{ and } \frac{7\pi}{6} < \beta < \frac{3\pi}{2}. \tag{B19}$$

$$z_j \sim -CA(\gamma, v), \quad \text{for } -\pi < \arg\{\gamma\} < -\frac{\pi}{2} \text{ and } -\frac{\pi}{2} < \beta < \frac{-\pi}{6};$$

$$z_j \sim C(A(\gamma, v) + B(\gamma, v)), \quad \text{for } -\pi < \arg\{\gamma\} < -\frac{\pi}{2} \text{ and } -\frac{\pi}{6} < \beta < \frac{\pi}{6}. \tag{B20}$$

If the first order complex turning point satisfies the second turning point condition, then the appropriate solution of equation (B9) follows.

- For left incidence boundary condition (turning point $j_{*2,l}$):

$$w_j \sim C\ (-A(\gamma, v) + B(\gamma, v)), \quad \text{for } -\pi < \arg\{\gamma\} < -\frac{\pi}{2} \text{ and } -\frac{\pi}{2} < \beta < \frac{-\pi}{6}; \tag{B21}$$

$$w_j \sim -CA(\gamma, v), \quad \text{for } -\pi < \arg\{\gamma\} < -\frac{\pi}{2} \text{ and } -\frac{\pi}{6} < \beta < \frac{\pi}{6};$$

$$w_j \sim C\ (A(\gamma, v) - B(\gamma, v)), \quad \text{for } \frac{\pi}{2} \arg\{\gamma\} \leqslant \pi \text{ and } \frac{5\pi}{6} < \beta < \frac{7\pi}{6}; \tag{B22}$$

$$w_j \sim CA(\gamma, v), \quad \text{for } \frac{\pi}{2} \arg\{\gamma\} \leqslant \pi \text{ and } \frac{7\pi}{6} < \beta < \frac{3\pi}{2}.$$

- For right incidence boundary condition (turning point $\bar{j}_{*2,l}$):

$$w_j \sim C\,(A(\gamma, v) + B(\gamma, v)), \quad \text{for } 0 \leqslant \arg\{\gamma\} < \frac{\pi}{2} \text{ and } \frac{\pi}{6} < \beta < \frac{\pi}{2}; \tag{B23}$$

$$w_j \sim C\,B(\gamma, v), \quad \text{for } 0 \leqslant \arg\{\gamma\} < \frac{\pi}{2} \text{ and } \frac{\pi}{6} < \beta < \frac{5\pi}{6};$$

$$w_j \sim C\,(A(\gamma, v) + B(\gamma, v)), \quad \text{for } 0 > \arg\{\gamma\} > -\frac{\pi}{2} \text{ and } \frac{\pi}{6} < \beta < \frac{\pi}{2} \tag{B24}$$

$$w_j \sim C\,B(\gamma, v), \quad \text{for } 0 > \arg\{\gamma\} > -\frac{\pi}{2} \text{ and } \frac{\pi}{2} < \beta < \frac{5\pi}{6}\ .$$

The next step is to match the asymptotic expansions, for $|\gamma| \to \infty$, of the appropriate solutions of the locally valid equations (32) and (B9) with the linear combination of expansions of the Liouville–Green functions in terms of the local variable α. The matching process is described in the next section.

B.2.2. *Matching process for complex first order turning points*

Here we describe how to match the expansion of the Liouville–Green functions in terms of the local variable α with the asymptotic expansion of the appropriate solution of the locally valid equations (32) and (B9), which were given in the previous section. First, we consider TPP1 (see box (A) of Figure 2) with turning points that satisfy the first turning point condition (30). The boundary conditions to consider follow below.

- Matching for the left incidence boundary condition. We have to match equation (B5), with equation (B16) if $0 < \arg\{\gamma\} < \pi/2$ with $\pi/2 < \beta < 5\pi/6$ or with equation (B17) if $0 \geqslant \arg\{\gamma\} > -\pi/2$ with $\pi/2 < \beta < 5\pi/6$. This matching gives

$$\frac{1}{2}\sqrt{\frac{\pi}{\gamma}}\,C = A\,\exp\left(\mathrm{i}\frac{\pi}{4} - \mathrm{i}I\,(a_l, r_l) - \mathrm{i}I\,(r_l, \bar{j}_{*1,l})\right), \tag{B25}$$

$$\frac{1}{2}\sqrt{\frac{\pi}{\gamma}}\,C = R^{-}A\exp\left(\mathrm{i}\frac{\pi}{4} + \mathrm{i}I\,(a_l, r_l) + \mathrm{i}I\,(r_l, \bar{j}_{*1,l})\right) \tag{B26}$$

  We have two equations and two unknowns, so we have the constants C and R^{-}. To obtain the transmission coefficient we need to match equation (B6) with equations (B16) or (B17), according to the value of $\arg\{\gamma\}$ and $\pi/6 < \beta < \pi/2$. This gives the transmission coefficient T^{-} in terms of the constant C given by equation (B25). The output of the matching process are the coefficients T^{-} and R^{-} given by equations (49) and (50).
- Matching for right incidence boundary condition. We have to match equation (B8), with equation (B19) with $3\pi/2 < \beta < 7\pi/6$ or equation (B20) with $-\pi/6 < \beta < \pi/6$, according to the value or $\arg\{\gamma\}$. This matching gives the coefficients C and R^{+}. To obtain the transmission coefficient we have to match equation (B7), with equation (B19) with $5\pi/6 < \beta < 3\pi/2$ or equation (B20) with $-\pi/2 < \beta < -\pi/6$, according to the value of $\arg\{\gamma\}$. This gives the

transmission coefficient T^+. The final result of this matching are the reflection R^+ and transmission T^+ coefficients given by equations (51) and (52).

Next we consider the right and left incidence boundary conditions for TPP1 with turning points that satisfies the second turning point condition (30).

- Matching for left incidence boundary condition. We match equation (B10), with equation (B21) with $-\pi/2 < \beta < -\pi/6$ or equation (B22) with $5\pi/6 < \beta < 7\pi/6$, according to the value of $\arg\{\gamma\}$. This matching gives the reflection coefficient R^- and the coefficient C. To obtain the transmission coefficient T^-, we match equation (B11) with equation (B21), with $-\pi/6 < \beta < \pi/6$ or equation (B22) with $7\pi/6 < \beta < 3\pi/2$, according to the value of $\arg\{\gamma\}$. The final result are the coefficients R^- and T^-, given by equations (53) and (54).
- Matching for right incidence boundary condition. We match equation (B13), with equation (B23), with $\pi/6 < \beta < \pi/2$, or equation (B24) with $\pi/6 < \beta < \pi/2$, according to the value of $\arg\{\gamma\}$. This matching gives the reflection coefficient R^+ and the coefficient C. To obtain the transmission coefficient T^+, we match equation (B12) with equation (B23), with $\pi/2 < \beta < 5\pi/6$, or equation (B24) with $\pi/2 < \beta < 5\pi/6$, according to the value of $\arg\{\gamma\}$. The final result are the coefficients R^+ and T^+, given by equations (55) and (56).

APPENDIX C: CONNECTION FORMULAE FOR A PAIR OF ALMOST COALESCING REAL AND COMPLEX FIRST ORDER TURNING POINTS

In this appendix, we describe how to obtain the connection formulae for TPP3 and TPP4. We also consider TPP5, which is the limiting case of TPP3 or TPP4. Results for TPP5 follow from the results for TPP3 or TPP4 by putting $b_{k,l} = 0$. First, we give the Liouville–Green functions in terms of the local variable α, defined for this case as

$$\alpha = -(-1)^k + \psi_{k,l}[(j - a_{k,l})^2 - b_{k,l}^2], \tag{C1}$$

where $a_{k,l}$ and $b_{k,l}$ for TPP3 are, respectively, the real and imaginary parts of a complex turning point that satisfies the kth turning point condition. In the case of TPP4, $a_{k,l}$ is the average of the two turning points and $b_{k,l}$ is half of the modulus of the difference between turning points.

C.1. APPROXIMATE FORM OF THE LIOUVILLE–GREEN FUNCTIONS

For TPP3 and TPP4 (see boxes (A) and (B) in Figure 2) we consider the boundary condition of left and right incidence. Here we give the appropriate linear combination of Liouville–Green functions in terms of the local variable α, given by equation (C1), that satisfy the boundary conditions mentioned above. We use the same notation as in section 4.4 regarding the reference points $r_{1,l}$ and $r_{2,l}$. For TPP3, we have $r_{1,l} = r_{2,l} = r_l$ (r_l is the real part of the pair of complex conjugate turning points). For TPP4, we have $r_{1,l} = j_{*k,l} < r_{2,l} = \hat{j}_{*k,l}$ ($j_{*k,l}$ and $\hat{j}_{*k,l}$ are the pair of real turning points). We define $f_l = r_l$ ($f_l = (j_{*k,l} + \hat{j}_{*k,l})/2$) when we consider TPP3 (TPP4).

- Left incidence boundary condition. We use the same notation as in section 4.4. The boundary points are $a_l < a_{l+1}$.

(1) For $a_l < j < r_{1,l}$ we have an incident plus a reflected wave:

$$z_j \sim A\, 2^{\mathrm{i}(3/4)\sqrt{\mu_{k,l}}(b_{k,l})^2 + (1/2)} (-1)^{-\mathrm{i}(1/8)\sqrt{\mu_{k,l}}(b_{k,l})^2} \mu_{k,l}^{-\mathrm{i}(1/8)\sqrt{\mu_{k,l}}(b_{k,l})^2 - 1/4} |j - f_l|^{-\mathrm{i}(1/4)\sqrt{\mu_{k,l}}(b_{k,l})^2 - 1/2}$$
$$\times \exp\left(-\mathrm{i}\frac{1}{4}\sqrt{\mu_{k,l}}|j - f_l|^2 - \mathrm{i}I(a_l, f_l) + \mathrm{i}\pi\, f_l \delta_{k,2}\right)$$
$$+ R^-\, A\; 2^{-\mathrm{i}(3/4)\sqrt{\mu_{k,l}}(b_{k,l})^2 + 1/2} (-1)^{+\mathrm{i}(1/8)\sqrt{\mu_{k,l}}(b_{k,l})^2} \mu_{k,l}^{\mathrm{i}(1/8)\sqrt{\mu_{k,l}}(b_{k,l})^2 - 1/4}$$
$$\times |j - f_l|^{\mathrm{i}(1/4)\sqrt{\mu_{k,l}}(b_{k,l})^2 - 1/2}$$
$$\times \exp\left(\mathrm{i}\frac{1}{4}\sqrt{\mu_{k,l}}|j - f_l|^2 + \mathrm{i}I(a_l, f_l) - \mathrm{i}\pi\, f_l \delta_{k,2}\right), \quad \text{as } j \to r_{1,l}^- \text{ and } b_{k,l} \to 0. \tag{C2}$$

(2) For $r_{2,l} < j < a_{l+1}$ we have a transmitted wave:

$$z_j \sim T^-\, A\; 2^{\mathrm{i}(3/4)\sqrt{\mu_{k,l}}(b_{k,l})^2 + 1/2} (-1)^{-\mathrm{i}(1/8)\sqrt{\mu_{k,l}}(b_{k,l})^2} \mu_{k,l}^{-\mathrm{i}(1/8)\sqrt{\mu_{k,l}}(b_{k,l})^2 - 1/4}$$
$$\times |j - f_l|^{-\mathrm{i}(1/4)\sqrt{\mu_{k,l}}(b_{k,l})^2 - 1/2} \times \exp\left(-\mathrm{i}\frac{1}{4}\sqrt{\mu_{k,l}}|j - f_l|^2 + \mathrm{i}\pi\, f_l \delta_{k,2}\right),$$
$$\text{as } j \to r_{2,l}^+ \text{ and } b_{k,l} \to 0. \tag{C3}$$

- Right incidence boundary condition. We use the same notation as for the left incidence boundary condition.

(1) For $a_l < j < r_{1,l}$ we have a transmitted wave:

$$z_j \sim T^+\, A\, 2^{-\mathrm{i}(3/4)\sqrt{\mu_{k,l}}(b_{k,l})^2 + 1/2} (-1)^{\mathrm{i}(1/8)\sqrt{\mu_{k,l}}(b_{k,l})^2} \mu_{k,l}^{\mathrm{i}(1/8)\sqrt{\mu_{k,l}}(b_{k,l})^2 - 1/4}$$
$$\times |j - f_l|^{\mathrm{i}(1/4)\sqrt{\mu_{k,l}}(b_{k,l})^2 - 1/2} \times \exp\left(\mathrm{i}\frac{1}{4}\sqrt{\mu_{k,l}}|j - f_l|^2 - \mathrm{i}\pi\, f_l \delta_{k,2}\right),$$
$$\text{as } j \to r_{1,l}^- \text{ and } b_{k,l} \to 0. \tag{C4}$$

(2) For $r_{2,l} < j < a_{l+1}$ we have an incident and a reflected wave:

$$z_j \sim A\; 2^{-\mathrm{i}(3/4)\sqrt{\mu_{k,l}}(b_{k,l})^2 + 1/2} (-1)^{\mathrm{i}(1/8)\sqrt{\mu_{k,l}}(b_{k,l})^2} \mu_{k,l}^{\mathrm{i}(1/8)\sqrt{\mu_{k,l}}(b_{k,l})^2 - (1/4)} |j - f_l|^{\mathrm{i}(1/4)\sqrt{\mu_{k,l}}(b_{k,l})^2 - 1/2}$$
$$\times \exp\left(\mathrm{i}\frac{1}{4}\sqrt{\mu_{k,l}}\,|j - f_l|^2 + \mathrm{i}I(a_{l+1}, f_l) - \mathrm{i}\pi\, f_l \delta_{k,2}\right)$$
$$+ R^+\, A\; 2^{+\mathrm{i}(3/4)\sqrt{\mu_{k,l}}(b_{k,l})^2 + 1/2} (-1)^{-\mathrm{i}(1/8)\sqrt{\mu_{k,l}}(b_{k\cdot l})^2} \mu_{k,l}^{-\mathrm{i}(1/8)\sqrt{\mu_{k,l}}(b_{k,l})^2 - 1/4}$$
$$\times |j - f_l|^{-\mathrm{i}(1/4)\sqrt{\mu_{k,l}}(b_{k,\,l})^2 - 1/2}$$
$$\times \exp\left(-\mathrm{i}\frac{1}{4}\sqrt{\mu_{k,l}}|j - f_l|^2 - \mathrm{i}I(a_{l+1}, f_l) + \mathrm{i}\pi\, f_l \delta_{k,2}\right),$$
$$\text{as } j \to r_{2,l}^+ \text{ and } b_{k,l} \to 0. \tag{C5}$$

For TPP5 (see box (C) of Figure 2), we just need to make $b_{k,l} = 0$ in the expressions above to obtain the linear combination of the Liouville–Green formulae in terms of the local variable α for the boundary conditions of left and right incidences.

C.2. ASYMPTOTIC EXPANSION OF THE SOLUTION OF THE APPROXIMATE EQUATION

The approximate equation for TPP3 or TPP4 is given by equation (35). This equation is related to the solutions of the Mathieu equation, so a closed-form solution is not available. We proceed to approximate equation (35) by a second order differential equation, as discussed in section 4.3.2. We obtain a differential equation which has a solution in terms of the parabolic cylinder functions. As a result, an approximate solution of the difference equation (35) is given by equations (42) and (43). In this section, we give the asymptotic expansion of the approximate solutions (42) and (43) for $|j - r_l| \gg 1$ (case TPP3, $r_l = \Re\{j_{*k,l}\}$) or $|j - (j_{*k,l} + \hat{j}_{*k,l})/2| \gg 1$ (case TPP4). The term $|j - r_l|$ appears in the asymptotic expansion of equations (42) and (43) when we have TPP3, and the term $|j - (j_{*k,l} + \hat{j}_{*k,l})/2|$ appears in the asymptotic expansion of equations (42) and (43) when we have TPP4. We define $f_l = r_l$ ($f_l = (j_{*k,l} + \hat{j}_{*k,l})/2$) if we consider TPP3 (TPP4). For TPP3 (TPP4), we have the asymptotic expansion for equations (42) and (43) that follows. In the expressions above, the upper (lower) sign is for the case TPP3 (TPP4):

$$
\begin{aligned}
z(j) \sim & \{A_1 (-1)^{\pm \mathrm{i}/4\sqrt{\mu_{k,l}}(b_{k,l})^2 - (1/2)} + B_1\} \exp\left(\pm \frac{\pi}{16} \sqrt{\mu_{k,l}} (b_{k,l})^2 + \mathrm{i}\,\frac{\pi}{8} \right. \\
& \left. + \frac{\sqrt{\mu_{k,l}}}{4} \mathrm{e}^{\mathrm{i}(\pi/2)} |j - f_l|^2 \right) \mu_{k,l}^{\pm \mathrm{i}/16\sqrt{\mu_{k,l}}(b_{k,l})^2 - (1/8)} |j - f_l|^{\pm \mathrm{i}/4\sqrt{\mu_{k,l}}(b_{k,l})^2 - (1/2)} - A_1 \\
& \times \frac{\sqrt{2\pi}}{\Gamma(\mp(\mathrm{i}/4)\sqrt{\mu_{k,l}}(b_{k,l})^2 + 1/2)} \exp\left(\mp \frac{5\pi}{16} \sqrt{\mu_{k,l}} (b_{k,l})^2 - \mathrm{i}\,\frac{3\pi}{8} \right. \\
& \left. + \frac{\sqrt{\mu_{k,l}}}{4} \mathrm{e}^{-\mathrm{i}(\pi/2)} |j - f_l^2| \right) (-1)^{\mp \mathrm{i}/4\sqrt{\mu_{k,l}}(b_{k,l})^2 - (1/2)} \mu_{k,l}^{\pm \mathrm{i}/16\sqrt{\mu_{k,l}}(b_{k,l})^2 - (1/8)} \\
& \times |j - f_l|^{\mp \mathrm{i}/4\sqrt{\mu_{k,l}}(b_{k,l})^2 - (1/2)}, \quad \text{as } |j - f_l| \gg 1 \text{ and } j - f_l < 0; \qquad \text{(C6)}
\end{aligned}
$$

$$
\begin{aligned}
z(j) \sim & \{B_1 (-1)^{\pm \mathrm{i}/4\sqrt{\mu_{k,l}}(b_{k,l})^2 - (1/2)} + A_1\} \exp\left(\pm \frac{\pi}{16} \sqrt{\mu_{k,l}} (b_{k,l})^2 + \mathrm{i}\,\frac{\pi}{8} \right) \\
& \times \mu_{k,l}^{\pm \mathrm{i}/16\sqrt{\mu_{k,l}}(b_{k,l})^2 - (1/8)} |j - f_l|^{\pm \mathrm{i}/4\sqrt{\mu_{k,l}}(b_{k,l})^2 - (1/2)} \exp\left(\frac{\mu_{k,l}^{1/2}}{4} \mathrm{e}^{\mathrm{i}(\pi/2)} |j - f_l|^2 \right) \\
& - B_1 \frac{\sqrt{2\pi}}{\Gamma(\mp(\mathrm{i}/4)\sqrt{\mu_{k,l}}(b_{k,l})^2 + 1/2)} \exp\left(\mp \frac{5\pi}{16} \sqrt{\mu_{k,l}} (b_{k,l})^2 - \mathrm{i}\,\frac{3\pi}{8} \right) \\
& \times (-1)^{\mp \mathrm{i}/4\sqrt{\mu_{k,l}}(b_{k,l})^2 - (1/2)} \mu_{k,l}^{\mp \mathrm{i}/16\sqrt{\mu_{k,l}}(b_{k,l})^2 - (1/8)} |j - f_l|^{\pm \mathrm{i}/4\sqrt{\mu_{k,l}}(b_{k,l})^2 - (1/2)}, \\
& \times \exp\left(\frac{\mu_{k,l}^{1/2}}{4} \mathrm{e}^{-\mathrm{i}(\pi/2)} |j - f_l|^2 \right), \quad \text{as } |j - f_l| \gg 1 \text{ and } j - f_l > 0. \qquad \text{(C7)}
\end{aligned}
$$

C.3. MATCHING PROCESS FOR A PAIR OF ALMOST COALESCING COMPLEX CONJUGATE FIRST ORDER TURNING POINTS

In this section, we describe the matching process which leads to the connection formulae for TPP3 (see Figure 2). We consider right and left incidence boundary conditions. We do not distinguish the connection formulae with respect to which conditions (30) are satisfied by the turning points. The connection formulae we discuss here are valid for turning points that satisfy the first or second turning point condition.

- Left incidence boundary condition. At first, we match the appropriate linear combination of the expansion of the Liouville–Green functions in terms of the local variable α, given by equation (C2) with the asymptotic expansion of the approximate solution of the locally valid difference equation, given by equation (C6). This matching results in two equations with three unknowns, namely, the reflection coefficient R^- and the coefficients A_1 and B_1. To obtain equations in terms of the coefficients A_1, B_1 and T^- (transmission coefficient), we match equation (C3) (expansion of the "transmitted wave" in terms of the local variable α) with equation (C7). Therefore, we have four equations and four unknowns. This system of equations leads to the reflection and transmission coefficients R^- and T^-, given by equations (61) and (62).
- Right incidence boundary condition. At first, we step match equation (C4) with the asymptotic expansion of the approximate solution of the locally valid difference equation, given by equation (C6). This matching results in two equations with three unknowns, namely, the transmission coefficient T^+ and the coefficients A_1 and B_1. To obtain equations in terms of the coefficients A_1, B_1 and R^+ (reflection coefficient), we match equation (C5) with equation (C7). Therefore, we have four equations and four unknowns. This system of equations leads to the reflection and transmission coefficients R^+ and T^+, given by equations (63) and (64).

C.4. MATCHING PROCESS FOR A PAIR OF ALMOST COALESCING REAL FIRST ORDER TURNING POINTS

We consider TPP4 (see Figure 2), with the turning points satisfying the first or second turning point condition (30). Besides this, we proceed in the same way as in the previous section.

- Left incidence boundary condition. At first, we match equation (C2) with equation (C6). The matching results in two equations with three unknowns, namely, the reflection coefficient R^- and the coefficients A_1 and B_1. To obtain equations in terms of the coefficients A_1, B_1 and T^-, we match equation (C3) with equation (C7). Therefore, we have four equations and four unknowns. This system of equations leads to the reflection and transmission coefficients R^- and T^-, given by equations (61) and (62).
- Right incidence boundary condition. At first, we match equation (C4) with equation (C6). The matching results in two equations with three unknowns,

namely the transmission coefficient T^+ and the coefficients A_1 and B_1. Second, we match equation (C5) with equation (C7) and obtain two equations in terms of the coefficients A_1, B_1 and T^+. Therefore, we have four equations and four unknowns. This system of equations leads to the reflection and transmission coefficients R^+ and T^+, given by equations (63) and (64).